

# Dirichlet eigenfunctions of the square membrane: Courant's property, and A. Stern's and Å. Pleijel's analyses

P. Bérard

Institut Fourier, Université de Grenoble and CNRS, B.P.74,  
F 38402 Saint Martin d'Hères Cedex, France.  
pierrehberard@gmail.com

and

B. Helffer

Laboratoire de Mathématiques, Univ. Paris-Sud and CNRS,  
F 91405 Orsay Cedex, France, and  
Laboratoire Jean Leray, Université de Nantes and CNRS  
F 44322 Nantes Cedex 3, France.  
Bernard.Helffer@math.u-psud.fr

March 11, 2015

To appear in Springer Proceedings in Mathematics & Statistics (2015), MIMS-GGTM conference in memory of M. S. Baouendi. Ali Baklouti, Aziz El Kacimi, Sadok Kallel, and Nordine Mir Editors.

To the memory of M. Salah Baouendi

## Abstract

In this paper, we revisit Courant's nodal domain theorem for the Dirichlet eigenfunctions of a square membrane, and the analyses of A. Stern and Å. Pleijel.

Keywords: Nodal lines, Nodal domains, Courant theorem.

MSC 2010: 35B05, 35P20, 58J50.

## 1 Introduction

Courant's celebrated nodal domain theorem [6] says that the number of nodal domains of an eigenfunction associated with a  $k$ -th eigenvalue of the Dirichlet Laplacian is less than or equal to  $k$ . Here, the eigenvalues are chosen to be positive, and listed in increasing order. It follows from a theorem of Pleijel [17] that equality in Courant's theorem only occurs for finitely many values of  $k$ . In this case, we speak of the Courant sharp situation. We refer to [11, 12] for the connection of this property with the question of minimal spectral partitions.

In the case of the square, it is immediate that the first, second and fourth eigenvalues are Courant sharp. In the first part of this note, Sections 2 and 3, we provide some missing arguments in Pleijel's paper leading to the conclusion that there are no other cases.

In the second part of this paper, we discuss some results of Antonie Stern. She was a PhD student of R. Courant, and defended her PhD in 1924, see [19, 20], and [21, p. 180]. In her thesis, she in particular provides an infinite sequence of Dirichlet eigenfunctions for the square, as well as an infinite sequence of spherical harmonics on the 2-sphere, which have exactly two nodal domains. In this paper, we focus on her results concerning the square, and refer to [3] for an analysis of the spherical case. In Section 4, we analyze Stern's argument, leading to the conclusion that her proofs are not quite complete. In Section 6, we provide a detailed proof of Stern's main result for the square, Theorem 4.1.

The authors would like to thank Virginie Bonnaillie-Noël for her pictures of nodal domains [5], and Annette Vogt for her biographical information on A. Stern. The authors are indebted to D. Jakobson for pointing out the unpublished report [10], and to M. Persson-Sundqvist for useful remarks. The authors thank the anonymous referee for his comments and careful reading. The second author would like to thank T. Hoffmann-Ostenhof for motivating discussions.

## 2 Pleijel's analysis

Consider the rectangle  $\mathcal{R}(a, b) = ]0, a\pi[ \times ]0, b\pi[$ . The Dirichlet eigenvalues for  $-\Delta$  are given by

$$\hat{\lambda}_{m,n} = \left( \frac{m^2}{a^2} + \frac{n^2}{b^2} \right), \quad m, n \geq 1,$$

with a corresponding basis of eigenfunctions given by

$$\phi_{m,n}(x, y) = \sin \frac{mx}{a} \sin \frac{ny}{b}.$$

It is easy to determine the Courant sharp eigenvalues when  $b^2/a^2$  is irrational (see for example [12]). The rational case is more difficult. Let us analyze the zero set of the Dirichlet eigenfunctions for the square. If we normalize the square as  $]0, \pi[ \times ]0, \pi[$ , we have,

$$\phi_{m,n}(x, y) = \phi_m(x)\phi_n(y), \quad \text{with } \phi_m(t) = \sin(mt).$$

Due to multiplicities, we have (at least) to consider the family of eigenfunctions,

$$(x, y) \mapsto \Phi_{m,n}(x, y, \theta) := \cos \theta \phi_{m,n}(x, y) + \sin \theta \phi_{n,m}(x, y),$$

with  $m, n \geq 1$ , and  $\theta \in [0, \pi[$ .

In [17], Pleijel claims that the Dirichlet eigenvalue  $\lambda_k$  of the square is Courant sharp if and only if  $k = 1, 2, 4$ . The key point in his proof is to exclude the eigenvalues  $\lambda_5, \lambda_7$  and  $\lambda_9$  which correspond respectively to the pairs  $(m, n) = (1, 3)$ ,  $(m, n) = (2, 3)$  and  $(m, n) = (1, 4)$ .

Let us briefly recall Pleijel's argument. Let  $N(\lambda) := \#\{n \mid \lambda_n < \lambda\}$  be the counting function. Using a covering of  $\mathbb{R}^2$  by the squares  $]k, k+1[ \times ]\ell, \ell+1[$ , he first establishes the estimate\*

$$N(\lambda) > \frac{\pi}{4}\lambda - 2\sqrt{\lambda} - 1. \quad (2.1)$$

---

\*There is an unimportant sign error in [17].

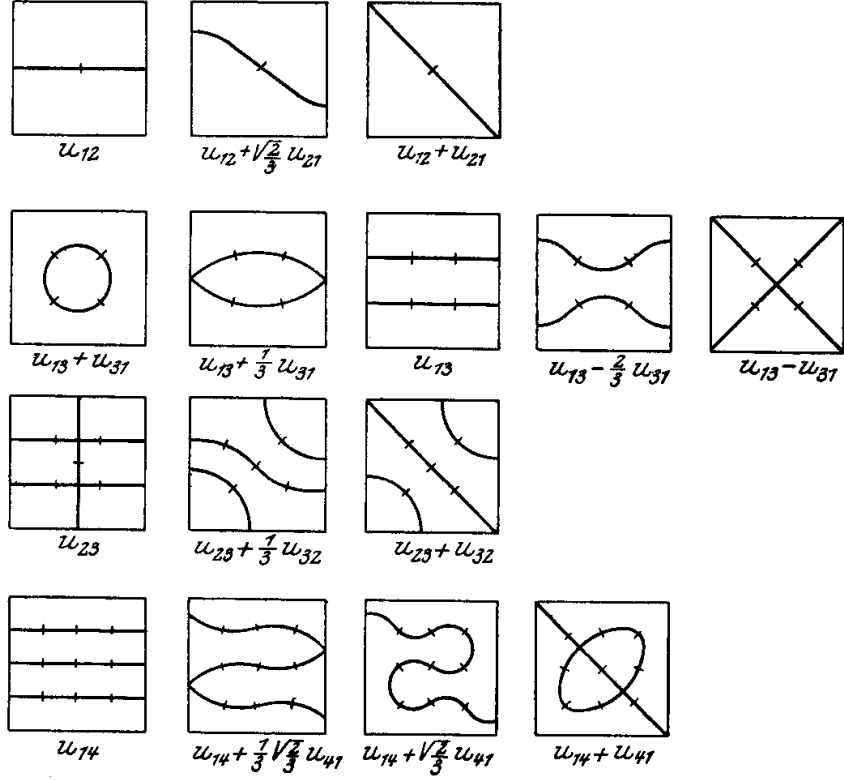


Figure 2.1: Nodal sets for the Dirichlet eigenvalues  $\lambda_2$ ,  $\lambda_5$ ,  $\lambda_7$  and  $\lambda_9$  (reproduced from [8])

If  $\lambda_n$  is Courant sharp, then  $\lambda_{n-1} < \lambda_n$ , hence  $N(\lambda_n) = n - 1$ , and

$$n > \frac{\pi}{4} \lambda_n - 2\sqrt{\lambda_n}. \quad (2.2)$$

On the other hand, if  $\lambda_n$  is Courant sharp, the Faber-Krahn inequality [1, 9] gives the necessary condition

$$\frac{\lambda_n}{n} \geq \frac{j_{0,1}^2}{\pi}$$

or

$$\frac{n}{\lambda_n} \leq \pi j_{0,1}^{-2} < 0.54323. \quad (2.3)$$

Recall that  $j_{0,1}$  is the smallest positive zero of the Bessel function of order 0, and that  $\pi j_{0,1}^2$  is the ground state energy of the disk of area 1.

Combining (2.2) and (2.3), leads to the inequality

$$\lambda_n \leq 68. \quad (2.4)$$

After re-ordering the values  $m^2 + n^2$ , we get the following spectral sequence for  $\lambda_n \leq 73$ ,

$$\begin{aligned}
\lambda_1 &= 2, & \lambda_2 &= \lambda_3 = 5, & \lambda_4 &= 8, & \lambda_5 &= \lambda_6 = 10, \\
\lambda_7 &= \lambda_8 = 13, & \lambda_9 &= \lambda_{10} = 17, & \lambda_{11} &= 18, & \lambda_{12} &= \lambda_{13} = 20, \\
\lambda_{14} &= \lambda_{15} = 25, & \lambda_{16} &= \lambda_{17} = 26, & \lambda_{18} &= \lambda_{19} = 29, & \lambda_{20} &= 32, \\
\lambda_{21} &= \lambda_{22} = 34, & \lambda_{23} &= \lambda_{24} = 37, & \lambda_{25} &= \lambda_{26} = 40, & \lambda_{27} &= \lambda_{28} = 41, \\
\lambda_{29} &= \lambda_{30} = 45, & \lambda_{31} &= \lambda_{32} = \lambda_{33} = 50, & \lambda_{34} &= \lambda_{35} = 52, & \lambda_{36} &= \lambda_{37} = 53, \\
\lambda_{38} &= \lambda_{39} = 58, & \lambda_{40} &= \lambda_{41} = 61, & \lambda_{42} &= \lambda_{43} = 65, & \lambda_{44} &= \lambda_{45} = 65, \\
\lambda_{46} &= \lambda_{47} = 68, & \lambda_{48} &= 72, & \lambda_{49} &= \lambda_{50} = 73, & \dots & .
\end{aligned} \tag{2.5}$$

It remains to analyze, among the eigenvalues which are less than or equal to 68, those which satisfy (2.3), and hence which can be Courant sharp. Computing the quotients  $\frac{n}{\lambda_n}$  in the list (2.5), leaves us with the eigenvalues  $\lambda_5$ ,  $\lambda_7$  and  $\lambda_9$ . For these last three cases, Pleijel refers to pictures in Courant-Hilbert [7], §V.5.3 p. 302, actually reproduced from [18], §II.B.6, p. 80, see Figure 2.1 in which  $u_{mn}(x, y)$  stands for  $\sin(mx) \sin(ny)$ . Although the details are not provided in these textbooks, the choice of the parameter values in the pictures suggests that some theoretical analysis is involved. It is however not clear whether the displayed nodal patterns represent all possible shapes, up to deformation or symmetries. The difficulty being that we have to analyze the nodal sets of eigenfunctions living in two-dimensional eigenspaces. Clearly,  $\phi_{m,n}$  has  $mn$  nodal components. This corresponds to the “product” situation with  $\theta = 0$  or  $\theta = \frac{\pi}{2}$ . The figures illustrate the fact that the number of nodal domains for a linear combination of two given independent eigenfunctions can be smaller or larger than the number of nodal domains of the given eigenfunctions. For these reasons, Pleijel’s argument does not appear fully convincing. In Section 3, we give a detailed proof that eigenvalues  $\lambda_5$ ,  $\lambda_7$  and  $\lambda_9$  are not Courant sharp.

**Remark.** As pointed out to us by M. Persson-Sundqvist, the last two cases can be easily dealt with using the following adaptation of an observation due to J. Leydold [14]. For any  $(m, n)$ ,

$$\Phi_{m,n}(\pi - x, \pi - y, \theta) = (-1)^{m+n} \Phi_{m,n}(x, y, \theta).$$

When  $(m+n)$  is odd, the corresponding eigenfunction function is odd under the symmetry with respect to the center of the square, and hence must have an even number of nodal domains. Our results are actually stronger, and describe the variation of the nodal sets.

### 3 The three remaining cases of Pleijel

Behind all the computations, we have the property that, for  $x \in ]0, \pi[$ ,

$$\sin mx = \sqrt{1 - u^2} U_{m-1}(u), \tag{3.1}$$

where  $U_{m-1}$  is the Chebyshev polynomial of second type and  $u = \cos x$ , see [15].

#### 3.1 First case : eigenvalue $\lambda_5$ , or $(m, n) = (1, 3)$ .

We look at the zeroes of  $\Phi_{1,3}(x, y, \theta)$ , see Figure 2.1, 2nd row. Since  $\Phi_{1,3}(x, y, \frac{\pi}{2} - \theta) = \Phi_{1,3}(y, x, \theta)$ , we can reduce the analysis of the nodal patterns to  $\theta \in [\frac{\pi}{4}, \frac{3\pi}{4}]$ . Let,

$$\cos x = u, \cos y = v. \tag{3.2}$$

This is a  $C^\infty$  change of variables from the square  $]0, \pi[ \times ]0, \pi[$  onto  $] -1, +1[ \times ] -1, +1[$ . In these coordinates, the zero set of  $\Phi_{1,3}(x, y, \theta)$  inside the square is given by

$$\cos \theta (4v^2 - 1) + \sin \theta (4u^2 - 1) = 0. \quad (3.3)$$

To completely determine the nodal set, we have to take the closure in  $[-1, 1] \times [-1, 1]$  of the zero set (3.3). The curve defined by (3.3) is an ellipse, when  $\theta \in [\frac{\pi}{4}, \frac{\pi}{2}[$ , a hyperbola, when  $\theta \in ]\frac{\pi}{2}, \frac{3\pi}{4}[$ , the union of two vertical lines, when  $\theta = \frac{\pi}{2}$ , the diagonals  $\{x - y = 0\} \cup \{x + y = 0\}$ , when  $\theta = \frac{3\pi}{4}$ . We only have to analyze how the ellipses and the hyperbolas are situated within the square.

**Boundary points.** At the boundary, for example on  $u = \pm 1$ , (3.3) gives:

$$\cos \theta (4v^2 - 1) + 3 \sin \theta = 0.$$

Depending on the value of  $\theta$ , we have no boundary point, the zero set (3.3) is an ellipse contained in the open square; one double boundary point, the zero set (3.3) is an ellipse, contained in the closed square, which touches the boundary at two points; or two boundary points, the zero set (3.3) is an ellipse or a hyperbola meeting the boundary of the square at four points.

**Interior critical points.** We now look at the critical points of the zero set of the function

$$\Psi_{1,3}(u, v, \theta) := \cos \theta (4v^2 - 1) + \sin \theta (4u^2 - 1).$$

We get two equations:

$$v \cos \theta = 0, \quad u \sin \theta = 0.$$

Except for the two easy cases when  $\cos \theta = 0$  or  $\sin \theta = 0$ , which can be analyzed directly (product situation), we immediately get that the only possible critical point is  $(u, v) = (0, 0)$ , i.e.,  $(x, y) = (\frac{\pi}{2}, \frac{\pi}{2})$ , and that this can only occur for  $\cos \theta + \sin \theta = 0$ , i.e., for  $\theta = \frac{3\pi}{4}$ .

The possible nodal patterns for an eigenfunction associated with  $\lambda_5$  all appear in Figure 2.1, second row.

This analysis shows rigorously that the number of nodal domains is 2, 3 or 4 as claimed in [17], and numerically observed in Figure 2.1. Observe that we have a rather complete description of the situation by analyzing the points at the boundary, and the critical points of the zero set inside the square. When no critical point or no change of multiplicity is observed at the boundary, the number of nodal domains remains constant. Hence, the complete computation could be done by analyzing the ‘‘critical’’ values of  $\theta$ , i.e., those for which there is a critical point on the zero set of  $\Psi_{1,3}$  in the interior, or a change of multiplicity at the boundary, and one ‘‘regular’’ value of  $\theta$  in each non critical interval. To explore all possible nodal patterns, and number of nodal domains, of the eigenfunctions  $\Phi_{1,3}^\theta$ ,  $\theta \in [\frac{\pi}{4}, \frac{3\pi}{4}]$ , associated with the eigenvalue  $\lambda_5$ , it is consequently sufficient to consider the values  $\theta = \frac{\pi}{4}$ ,  $\theta = \arctan 3$ ,  $\theta = \frac{\pi}{2}$ ,  $\theta = \frac{3\pi}{4}$ .

### 3.2 Second case: eigenvalue $\lambda_7$ , or $(m, n) = (2, 3)$ .

We look at the zeros of  $\Phi_{2,3}(x, y, \theta)$ . We first observe that

$$\Phi_{2,3}(x, y, \theta) = \sin x \sin y (2 \cos \theta \cos x (\cos 2y + 2 \cos^2 y) + 2 \sin \theta \cos y (\cos 2x + 2 \cos^2 x)).$$

In the coordinates (3.2), this reads:

$$\Phi_{2,3}(x, y, \theta) = 2\sqrt{1-u^2}\sqrt{1-v^2} (u \cos \theta(4v^2 - 1) + v \sin \theta(4u^2 - 1)). \quad (3.4)$$

We have to look at the solutions of

$$\Psi_{2,3}(u, v, \theta) := u(4v^2 - 1) \cos \theta + v(4u^2 - 1) \sin \theta = 0, \quad (3.5)$$

inside  $[-1, +1] \times [-1, +1]$ .

**Analysis at the boundary.** The function  $\Psi_{2,3}$  is anti-invariant under the change  $(u, v) \rightarrow (-u, -v)$ . Changing  $u$  into  $-u$  amounts to changing  $\theta$  in  $\pi - \theta$ . Exchanging  $(x, y)$  into  $(y, x)$  amounts to changing  $\theta$  into  $\frac{\pi}{2} - \theta$ . This implies that it suffices to consider the values  $\theta \in [0, \frac{\pi}{2}]$ , and the boundaries  $u = -1$  and  $v = -1$ . At the boundary  $u = -1$ , we get:

$$-\cos \theta(4v^2 - 1) + 3v \sin \theta = 0, \quad (3.6)$$

with the condition that  $v \in [-1, +1]$ .

We note that the product of the roots is  $-\frac{1}{4}$ , and that there are always two distinct solutions in  $\mathbb{R}$ . For  $\theta = 0$ , we have two solutions given by  $v = \pm \frac{1}{2}$ . When  $\theta$  increases we still have two solutions in  $[-1, 1]$  till the largest one is equal to 1 (the other one being equal to  $-\frac{1}{4}$ ). This is obtained for  $\theta = \frac{\pi}{4}$ . For  $\theta > \frac{\pi}{4}$ , there is only one negative solution in  $[-1, 1]$ , tending to zero as  $\theta \rightarrow \frac{\pi}{2}$ .

At the boundary  $v = -1$ , we have for  $\theta = 0$ ,  $u = 0$  as unique solution. When  $\theta$  increases, there is only one solution in  $[-1, 1]$ , till  $\frac{\pi}{4}$ , where we get two solutions  $u = -\frac{1}{4}$  and  $u = 1$ . For this value of  $\theta$ , the zero set is given by  $(u + v)(4uv - 1) = 0$ . For  $\theta \in ]\frac{\pi}{4}, \frac{\pi}{2}]$ , we have two solutions.

We conclude that the zero set of  $\Psi_{2,3}$  always hits the boundary at six points.

**Critical points.** We now look at the critical points of  $\Psi_{2,3}$ . We get two equations:

$$(4v^2 - 1) \cos \theta + 8uv \sin \theta = 0, \quad (3.7)$$

and

$$8uv \cos \theta + (4u^2 - 1) \sin \theta = 0. \quad (3.8)$$

The critical points on the zero set of  $\Psi_{2,3}$  are the common solutions of (3.5), (3.7), and (3.8).

If  $\cos \theta \sin \theta \neq 0$ , we immediately obtain that  $u = v = 0$ , and these equations have no common solution. It follows that the eigenfunctions associated with  $\lambda_7$  have no interior critical point on their nodal sets.

One can give the following expressions for the partial derivatives of  $\Psi_{2,3}$ ,

$$\partial_u \Psi_{2,3}(u, v, \theta) = \frac{v}{u}(4u^2 + 1) \sin \theta \quad \text{and} \quad \partial_v \Psi_{2,3}(u, v, \theta) = \frac{u}{v}(4v^2 + 1) \cos \theta,$$

for  $u$ , resp.  $v$ , different from 0. Since a regular closed curve contains points with vertical or horizontal tangents, it follows that the zero set of  $\Psi_{2,3}$  cannot contain any closed component (necessarily without self-intersections, otherwise the nodal set of  $\Phi_{2,3}$  would have a critical point). The components of this zero set are lines joining two boundary points which are decreasing from the left to the right. These lines cannot intersect each other (for the same reason as before).

The possible nodal patterns for an eigenfunction associated with  $\lambda_7$  all appear in Figure 2.1, third row.

The number of nodal domains is four (delimited by three non intersecting lines) or six in the product case. Hence the maximal number of nodal domains is six.

### 3.3 Third case : eigenvalue $\lambda_9$ , or $(m, n) = (1, 4)$

We look at the zeros of  $\Phi_{1,4}(\cdot, \cdot, \theta)$ . Here we can write

$$\Phi_{1,4}(x, y, \theta) = 4 \sin x \sin y \Psi_{1,4}(u, v, \theta)$$

with

$$\Psi_{1,4}(u, v, \theta) := \cos \theta v(2v^2 - 1) + \sin \theta u(2u^2 - 1).$$

Hence, we have to analyze the equation

$$\cos \theta v(2v^2 - 1) + \sin \theta u(2u^2 - 1) = 0. \quad (3.9)$$

Notice that the functions  $\Psi_{1,4}(u, v, \theta)$  are anti-invariant under the symmetry  $(u, v) \rightarrow (-u, -v)$ , and that one can reduce from  $\theta \in [0, \pi[$  to the case  $\theta \in [0, \frac{\pi}{2}]$  by making use of the symmetries with respect to the lines  $\{u = 0\}$ ,  $\{v = 0\}$  and  $\{u = v\}$ . One can even reduce the analysis to  $\theta \in [0, \frac{\pi}{4}]$  by changing  $\theta$  into  $\frac{\pi}{2} - \theta$ , and  $(x, y)$  into  $(y, x)$ .

**Boundary points.** Due to the symmetries, the zero set of  $\Psi_{1,4}$  hits parallel boundaries at symmetrical points. For  $u = \pm 1$  these points are given by:

$$v(2v^2 - 1) \pm \tan \theta = 0.$$

If we start from  $\theta = 0$ , we first have three zeroes, corresponding to points at which the zero set of  $\Psi_{1,4}$  arrives at the boundary:  $0, \pm \frac{1}{\sqrt{2}}$ . Looking at the derivative, we have a double point when  $v = \pm \frac{1}{\sqrt{6}}$ , which corresponds to  $\tan \theta = \frac{\sqrt{2}}{3\sqrt{3}}$ . For larger values of  $\theta$ , we have only one point till  $\tan \theta = 1$ .

Hence, there are 3, 2, 1 or 0 solutions satisfying  $v \in [-1, +1]$ . The analogous equation for  $v = \pm 1$  appears with  $\cot \theta$  instead of  $\tan \theta$ , so that the boundary analysis depends on the comparison of  $|\tan \theta|$  with  $\frac{\sqrt{2}}{3\sqrt{3}}$ , 1 and  $\frac{3\sqrt{3}}{\sqrt{2}}$ . When the points disappear on  $u = \pm 1$ , they appear on  $v = \pm 1$ . Notice that the value  $\frac{\sqrt{2}}{3\sqrt{3}}$  appears in Figure 2.1 and in Courant-Hilbert's book [7], §V.5.3, p. 302. Finally, the maximal number of points along the boundary is six, counting multiplicities.

**Critical points.** The critical points of  $\Psi_{1,4}$  satisfy:

$$\cos \theta (6v^2 - 1) = 0, \quad (3.10)$$

and

$$\sin \theta (6u^2 - 1) = 0. \quad (3.11)$$

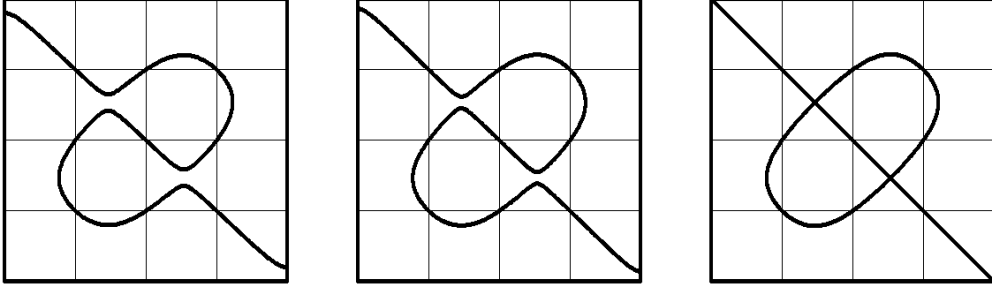


Figure 3.1: Eigenvalue  $\lambda_9$ , deformation of the nodal set near  $\theta = \frac{\pi}{4}$

If we exclude the “product” case, the only critical points are determined by  $u^2 = \frac{1}{6}$  and  $v^2 = \frac{1}{6}$ . Plugging these values in (3.9), we obtain that interior critical points on the zero set of  $\Psi_{1,4}$  can only appear when:

$$\cos \theta \pm \sin \theta = 0. \quad (3.12)$$

Hence, we only have to look at  $\theta = \frac{\pi}{4}$  and  $\theta = \frac{3\pi}{4}$ . Because of symmetries, it suffices to consider the case  $\theta = \frac{\pi}{4}$ :

$$\Psi_{1,4}(u, v, \frac{\pi}{4}) := \frac{1}{\sqrt{2}}(v(2v^2 - 1) + u(2u^2 - 1)) = \frac{1}{\sqrt{2}}(u + v)(2(u - \frac{v}{2})^2 + \frac{3}{2}v^2 - 1).$$

The zero set is the union of an ellipse contained in the square, and the anti-diagonal, with two intersection points. It follows that the function  $\Phi_{1,4}(x, y, \frac{\pi}{4})$  has four nodal domains. Figure 3.1 shows the deformation of the nodal set of  $\Phi_{1,4}(x, y, \theta)$  for  $\theta \leq \frac{\pi}{4}$  close to  $\frac{\pi}{4}$ , as well as the grid  $\{\sin(4x)\sin(4y) = 0\}$ . Figure 3.2 shows the deformation for  $\Phi_{1,6}(x, y, \theta)$ .

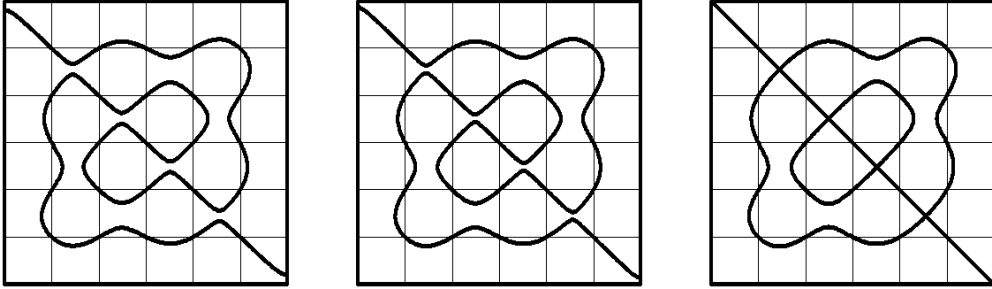


Figure 3.2: Eigenvalue  $\lambda_{23}$ , deformation of the nodal set near  $\theta = \frac{\pi}{4}$

Let us summarize what we have so far obtained for the eigenfunctions associated with  $\lambda_9$ .

- We have determined the shape of the nodal set of  $\Phi_{1,4}$  when  $\theta = \frac{\pi}{4}$  or  $\frac{3\pi}{4}$ , and we can easily see that these are the only cases in which the interior part of the nodal set hits the boundary at the vertices.
- When  $\theta \neq \frac{\pi}{4}$  or  $\frac{3\pi}{4}$ , we have proved that the nodal set of  $\Phi_{1,4}$  has no interior critical point, hence no self-intersection, and that it hits the boundary at 2 or 6 points, counting multiplicities.



- We can also observe that all nodal sets must contain the lattice points  $(i\frac{\pi}{4}, j\frac{\pi}{4})$  for  $1 \leq i, j \leq 3$ , and that these points are always regular points of the nodal sets. This implies, by energy considerations, that the nodal sets cannot contain any closed component avoiding these lattice points. The lattice points are indicated in Figure 2.1. They appear in Figures 3.1 and 3.1 as the vertices of the grids.

We still need to prove that all the possible nodal patterns for an eigenfunction associated with the eigenvalue  $\lambda_9$  appear in Figure 2.1, fourth row, and hence that the maximal number of nodal domains is 4, so that  $\lambda_9$  is not Courant sharp. When  $\theta \in [0, \frac{\pi}{4}]$ , this can be done by looking at the intersections of the nodal sets with the horizontal lines  $\{y = \arccos(\pm\sqrt{\frac{1}{6}})\}$ . We leave the details to the reader, and refer to Section 6 for general arguments.

**Remark.** Figure 2.1 and 3.1 indicate that for some values of  $\theta$ , the function  $\Phi_{1,4}(x, y, \theta)$  has exactly two nodal domains. This phenomenon has been studied by Antonie Stern [19] who claims that for any  $k \geq 2$ , there exists an eigenfunction associated with the Dirichlet eigenvalue  $(1 + 4k^2)$  of the square  $[0, \pi]^2$ , with exactly two nodal domains. In Sections 4 – 6, we look at Stern’s thesis more carefully.

## 4 The observations of A. Stern

The general topic of A. Stern’s thesis [19] is the asymptotic behaviour of eigenvalues and eigenfunctions. In Part I, she studies the nodal sets of eigenfunctions of the Laplacian in the square with Dirichlet boundary condition, and on the 2-sphere. The eigenvalues are chosen to be positive, and listed in increasing order, with multiplicities. In [20], we propose extracts from Stern’s thesis, with annotations and highlighting to point out the main results and ideas.

As we have seen in the previous sections, Pleijel’s theorem [17] states that for a plane domain, there are only finitely many Courant sharp Dirichlet eigenvalues. For the Dirichlet Laplacian in the square, A. Stern claims [20, tags E1, Q1] that there are actually infinitely many eigenfunctions having exactly two nodal domains,

[E1]...Im eindimensionalen Fall wird nach den Sätzen von Sturm<sup>†</sup> das Intervall durch die Knoten der  $n$ ten Eigenfunktion in  $n$  Teilgebiete zerlegt. Dies Gesetz verliert seine Gültigkeit bei mehrdimensionalen Eigenwertproblemen, ... es läßt sich beispielweise leicht zeigen, daß auf der Kugel bei jedem Eigenwert die Gebietszahlen 2 oder 3 auftreten, und daß bei Ordnung nach wachsenden Eigenwerten auch beim Quadrat die Gebietszahl 2 immer wieder vorkommt.

[Q1]... Wir wollen nun zeigen, daß beim Quadrat die Gebietszahl zwei immer wieder auftritt.

The second statement is mentioned in the book of Courant-Hilbert [7], §VI.6, p. 455.

Pleijel’s theorem has been generalized to surfaces by J. Peetre [16], see also [4]. As a consequence, only finitely many eigenvalues of the sphere are Courant sharp. A. Stern claims [20, tags E1, K1, K2] that, for any  $\ell \geq 2$ , there exists a spherical harmonic of degree  $\ell$  with exactly three nodal domains when  $\ell$  is odd, *resp.* with exactly two nodal domains when  $\ell$  is even,

---

<sup>†</sup>Journal de Mathématiques, T.1, 1836, p. 106-186, 269-277, 375-444

[K1] ... Zunächst wollen wir zeigen, daß es zu jedem Eigenwert Eigenfunktionen gibt, deren Nulllinien die Kugelfläche nur in zwei oder drei Gebiete teilen.

[K2] ... Die Gebietszahl zwei tritt somit bei allen Eigenwerten  $\lambda_n = (2r + 1)(2r + 2)$   $r = 1, 2, \dots$  auf; ebenso wollen wir jetzt zeigen, daß die Gebietszahl drei bei allen Eigenwerten

$$\lambda_n = 2r(2r + 1) \quad r = 1, 2, \dots$$

immer wieder vorkommt.

These two statements are usually attributed to H. Lewy [13].

In this paper, we shall only deal with the case of the square, leaving the case of the sphere for [3]. First, we quote the main statements made by A. Stern [20, tags Q1-Q3], and summarize them in Theorem 4.1.

[Q2]... Wir betrachten die Eigenwerte

$$\lambda_n = \lambda_{2r,1} = 4r^2 + 1, \quad r = 1, 2, \dots$$

und die Knotenlinie der zugehörige Eigenfunktion

$$u_{2r,1} + u_{1,2r} = 0,$$

für die sich, wie leicht mittels graphischer Bilder nachgewiesen werden kann, die Figur 7 ergibt.

[Q3]... Laßen wir nur  $\mu$  von  $\mu = 1$  aus abnehmen, so lösen sich die Doppelpunkte der Knotenlinie alle gleichzeitig und im gleichem Sinne auf, und es ergibt sich die Figur 8. Da die Knotenlinie aus einem Doppelpunktlosen Zuge besteht, teilt sich das Quadrat in zwei Gebiete und zwar geschieht dies für alle Werte  $r = 1, 2, \dots$ , also Eigenwerte  $\lambda_n = \lambda_{2r,1} = 4r^2 + 1$ .

**Theorem 4.1** *For any  $r \in \mathbb{N}$ , consider the family  $\Phi_{1,2r}(x, y, \theta)$  of eigenfunctions of the Laplacian in the square  $[0, \pi]^2$ , associated with the Dirichlet eigenvalue  $1 + 4r^2$ ,*

$$\Phi_{1,2r}^\theta(x, y) := \Phi_{1,2r}(x, y, \theta) := \cos \theta \sin x \sin(2ry) + \sin \theta \sin(2rx) \sin y.$$

Then,

- (i) for  $\theta = \frac{\pi}{4}$ , the nodal pattern of  $\Phi$  is as shown in Figure 4.1, left, [19, Fig. 7];
- (ii) for  $\theta < \frac{\pi}{4}$ , and  $\theta$  sufficiently close to  $\frac{\pi}{4}$ , the double points all disappear at the same time and in a similar manner ('im gleichem Sinne') as in Figure 4.1, right, [19, Fig. 8]. The nodal set consists of a connected line ('aus einem Zuge') with no double point. It divides the square into two domains.

**Remark.** Although this is not stated explicitly, one can infer from Stern's thesis, (i) that the eigenfunction  $\Phi_{1,2r}(x, y, \frac{\pi}{4})$  has  $2r$  nodal domains and  $(2r - 2)$  double points, and (ii) that for  $\theta$  close to and different from  $\frac{\pi}{4}$ , the nodal set of  $\Phi_{1,2r}(x, y, \theta)$  consists of the boundary of the square and a *connected* simple curve from one point of the boundary to a symmetric point. This curve divides the domain into two connected components.

A. Stern states two simple properties which play a key role in the proofs [20, tags I1, I2]. These statements are formalized in Properties 4.2 below.

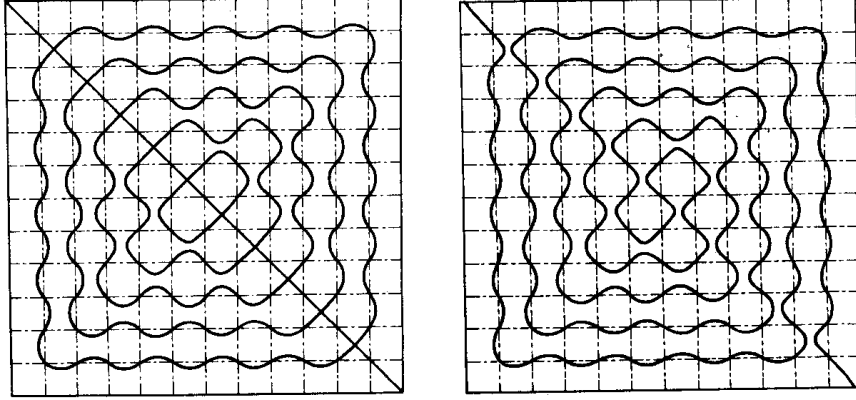


Figure 4.1: Case  $r = 6$ , nodal sets for  $\theta = \frac{\pi}{4}$  and  $\theta$  close to  $\frac{\pi}{4}$  (reproduced from [8])

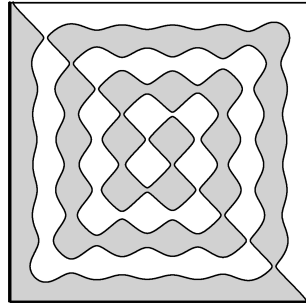


Figure 4.2: Nodal domains, courtesy Virginie Bonnaillie-Noël [5]

[I1]... Um den typischen Verlauf der Knotenlinie zu bestimmen, haben wir ähnliche Anhaltspunkte wie auf der Kugelfläche. Legen wir die Knotenliniensysteme von  $u_{\ell,m}$  ( $\ell - 1$  Parallelen zur  $y$ -Achse,  $m - 1$  zur  $x$ -Achse) und  $u_{m,\ell}$  ( $m - 1$  Parallelen zur  $y$ -Achse,  $\ell - 1$  zur  $x$ -Achse) übereinander, so kann für  $\mu > 0$  ( $< 0$ ) die Knotenlinie nur in den Gebieten verlaufen, in denen beide Funktionen verschiedenes (gleiches) Vorzeichen haben.

[I2]... Weiter müssen alle zum Eigenwert  $\lambda_{n,m}$  gehörigen Knotenlinien durch Schnittpunkte der Liniensysteme  $u_{\ell,m} = 0$  und  $u_{m,\ell} = 0$ , also durch  $(\ell - 1)^2 + (m - 1)^2$  feste Punkte hindurchgehen ...

**Properties 4.2** Let  $\phi$  and  $\psi$  be two linearly independent eigenfunctions associated with the same eigenvalue for the square  $\mathcal{S}$ . Let  $\mu$  be a real parameter, and consider the family of eigenfunctions  $\phi_\mu = \psi + \mu\phi$ . Let  $N(\phi)$  denote the nodal set of the eigenfunction  $\phi$ .

(i) Consider the domains in  $\mathcal{S} \setminus N(\phi) \cup N(\psi)$  in which  $\mu\phi\psi > 0$  and hatch them<sup>‡</sup>. Then the nodal set  $N(\phi_\mu)$  avoids the hatched domains.

(ii) The points in  $N(\phi) \cap N(\psi)$  belong to the nodal set  $N(\phi_\mu)$  for all  $\mu$ .

<sup>‡</sup>‘schraffieren’, see [20, tag I1], in the spherical case.

**Property 4.3** *The nodal set  $N(\phi_\mu)$  depends continuously on  $\mu$ .*

**Remark.** As a matter of fact, A. Stern uses Property 4.2 in both cases (square and sphere), and only mentions Property 4.3 in the case of the sphere. She says nothing on the proof of this second property which is more or less clear near regular points, but not so clear near multiple points. H. Lewy provides a full proof in the case of the sphere [13, Lemmas 2-4].

Finally, A. Stern mentions that she uses a graphical method (‘mittels graphischer Bilder’ and ‘unter Zuhilfenahme graphischer Bilder’ [20, tags Q2, Q4]) which may have been classical at her time, and could explain the amazing quality of her pictures. On this occasion, she mentions a useful idea in her § I.3, namely looking at the intersections of the nodal set  $N(\phi_\mu)$  with horizontal or vertical lines.

All in all, the arguments given by A. Stern seem rather sketchy to us, and we do not think that they are quite sufficient to conclude the proof of Theorem 4.1.

In our opinion, taking care of the following items is missing in Stern’s thesis.

- (i) Complete determination of the multiple points of  $N(\Phi^{\frac{\pi}{4}})$  ;
- (ii) Absence of multiple points in  $N(\Phi^\theta)$ , when  $\theta$  is different from  $\frac{\pi}{4}$ , and close to  $\frac{\pi}{4}$  ;
- (iii) Connectedness of the nodal set  $N(\Phi^\theta)$ , or why there are no other components, e.g. closed inner components, in the nodal set.

The aim of this paper is to complete the proofs of A. Stern in the case of the square.

**Remark.** In [13], H. Lewy gives a complete proof of Stern’s results <sup>§</sup> in the case of the sphere. In the unpublished preprint [10], the authors provide partial answers to the above items in the case of the square.

The key steps to better understand the possible nodal patterns for the eigenvalues  $1 + 4r^2$  (and other eigenvalues as well), and to answer the above items, are the following.

- Subsection 6.3, in which we study the points which are both zeroes and critical points of the functions  $\Phi_{1,R}^\theta$ .
- Subsection 6.4, in which we study the possible local nodal patterns of the functions  $\Phi_{1,R}^\theta$ .
- Subsection 6.5, in which we determine the nodal sets of the functions  $\Phi_{1,R}^\theta$  for  $\theta = \frac{\pi}{4}$  or  $\frac{3\pi}{4}$ .

In the subsequent subsections, we study the deformation of the nodal set of  $\Phi_{1,R}^\theta$  when  $\theta$  varies close to  $\frac{\pi}{4}$  or  $\frac{3\pi}{4}$ , and conclude the proof of Theorem 4.1. As a matter of fact, our approach gives the maximal interval in which the nodal set of  $\Phi_{1,R}^\theta$  remains connected, without critical points, see Lemma 6.10 (i).

**Sketch of the proof of Theorem 4.1.** Consider the eigenvalue  $\hat{\lambda}_{1,R} := 1 + R^2$  for the square  $\mathcal{S} := ]0, \pi[^2$  with Dirichlet boundary conditions, and consider the eigenfunction

$$\Phi^\theta(x, y) := \Phi(x, y, \theta) := \cos \theta \sin x \sin(Ry) + \sin \theta \sin(Rx) \sin y, \quad \theta \in [0, \pi[.$$

---

<sup>§</sup> A. Stern and H. Lewy were both students of R. Courant at about the same time, 1925. H. Lewy does however not refer to A. Stern’s Thesis in his paper. We refer to [3] for a further discussion.

Let us introduce the  $Q$ -squares,

$$Q_{i,j} := ]\frac{i\pi}{R}, \frac{(i+1)\pi}{R}[\times]\frac{j\pi}{R}, \frac{(j+1)\pi}{R}[, \text{ for } 0 \leq i, j \leq R-1,$$

and the lattice,

$$\mathcal{L} := \left\{ \left( \frac{i\pi}{R}, \frac{j\pi}{R} \right) \mid 1 \leq i, j \leq R-1 \right\}.$$

The basic idea is to start from the analysis of a given nodal set, e.g. from the nodal set  $N(\Phi^{\frac{\pi}{4}})$ , and then to use some kind of perturbation argument.

Here are the key points.

- (i) Use Property 4.2: Assertion (i) defines checkerboards by  $Q$ -squares (depending on the sign of  $\cos \theta$ ), whose grey squares do not contain any nodal point of  $\Phi^\theta$ . Assertion (ii) says that the lattice  $\mathcal{L}$  is contained in the nodal set  $N(\Phi^\theta)$  for all  $\theta$ .
- (ii) Determine the possible *critical zeroes* of the eigenfunction  $\Phi^\theta$ , i.e., the zeroes which are also critical points, both in the interior of the square or on the boundary. They indeed correspond to multiple points in the nodal set. Note that the points in  $\mathcal{L}$  are not critical zeroes, see Subsection 6.3.
- (iii) Determine whether critical zeroes are degenerate or not and their order when they are degenerate.
- (iv) Determine how critical zeroes appear or disappear when  $\theta$  varies, and how the nodal set  $N(\Phi^\theta)$  evolves. For this purpose, make a local analysis in the square  $Q_{i,j}$ , depending on whether it is contained in  $\mathcal{S}$  or touches the boundary, see Subsection 6.4.
- (v) Determine the nodal sets of the eigenfunctions  $Z_\pm$  associated with the eigenvalue  $\hat{\lambda}_{1,R}$ . For this purpose, determine precisely the critical zeroes of  $\Phi^\theta$  for  $\theta = \frac{\pi}{4}$  and  $\frac{3\pi}{4}$ , and prove a separation lemma in the  $Q_{i,j}$  to determine whether the medians of this  $Q$ -square meet the nodal set of  $\Phi^\theta$  when  $\theta = \frac{\pi}{4}$  or  $\frac{3\pi}{4}$ , see Subsection 6.4.
- (vi) Prove that the nodal set  $N(\Phi^\theta)$  does not contain any closed component.

Take  $R = 2r$  and  $0 < \frac{\pi}{4} - \theta \ll 1$ . Using the above analysis one can actually give a complete proof of Theorem 4.1. The analysis of the local possible nodal patterns shows that the nodal set  $N(\Phi^{\frac{\pi}{4}})$  is indeed as stated. For  $0 < \frac{\pi}{4} - \theta \ll 1$ , the eigenfunction  $\Phi^\theta$  has no critical zero in  $\mathcal{S}$ , and exactly two critical zeroes on the boundary, symmetric with respect to the center of the square. This proves in particular that the critical zeroes of  $\Phi^{\frac{\pi}{4}}$  all disappear at once when  $\theta$  changes,  $\theta < \frac{\pi}{4}$ . Starting from one of the critical zeroes on the boundary, and using the above analysis, one can actually follow a connected nodal simple curve passing through all the points in  $\mathcal{L}$  and going from one of the critical zeroes on the boundary to the second one. To finish the proof it suffices to show that there are no other component of  $N(\Phi^\theta)$  in  $\mathcal{S}$ .

## 5 Notation and definitions. General properties of the nodal sets.

### 5.1 Notation and definitions, I.

Let  $\mathcal{S}$  be the open square  $]0, \pi[^2$  in the plane. We denote by  $\partial\mathcal{S}$  boundary, by  $\mathcal{D}_+$  the diagonal, by  $\mathcal{D}_-$  the anti-diagonal, and by  $O := (\frac{\pi}{2}, \frac{\pi}{2})$  the center of  $\mathcal{S}$ .

Let  $\Phi$  be an eigenfunction for the Dirichlet Laplacian in  $\mathcal{S}$ . We let

$$N(\Phi) := \{(x, y) \in \overline{\mathcal{S}} \mid \Phi(x, y) = 0\} \quad (5.1)$$

denote the nodal set of  $\Phi$ , and

$$N_i(\Phi) := N(\Phi) \cap \mathcal{S} \quad (5.2)$$

denote the interior part of  $N(\Phi)$ .

Given two integers  $m, n \geq 1$ , we consider the one-parameter family of eigenfunctions,

$$\Phi_{m,n}^\theta(x, y) := \Phi_{m,n}(x, y, \theta) := \cos \theta \sin(mx) \sin(ny) + \sin \theta \sin(nx) \sin(my), \quad (5.3)$$

with  $x, y \in [0, \pi]$  and  $\theta \in [0, \pi[$ .

Unless necessary, we skip the index  $(m, n)$ . These eigenfunctions are associated with the eigenvalue

$$\hat{\lambda}_{m,n} := m^2 + n^2. \quad (5.4)$$

The following eigenfunctions are of particular interest.

$$\begin{aligned} X &:= \Phi^0, & Y &:= \Phi^{\frac{\pi}{2}}, \\ Z_+ &:= \Phi^{\frac{\pi}{4}}, & Z_- &:= \Phi^{\frac{3\pi}{4}}. \end{aligned} \quad (5.5)$$

Denote by

$$\mathcal{L} := N_i(X) \cap N_i(Y), \quad (5.6)$$

the set of zeroes which are common to all eigenfunctions  $\Phi^\theta, \theta \in [0, \pi[$ .

**Definition 5.1** *A critical zero of  $\Phi$  is a point  $(x, y) \in \overline{\mathcal{S}}$  such that both  $\Phi$  and  $\nabla\Phi$  vanish at  $(x, y)$ .*

### 5.2 General properties of nodal sets.

Although stated in the case of the square, the following properties are quite general (see [2] and references therein) for eigenfunctions of the Dirichlet realization of the Laplacian in a regular domain of  $\mathbb{R}^2$ .

**Properties 5.2** *Let  $(x, y)$  be a point in  $\mathcal{S}$  (an interior point).*

- (i) *A non-zero eigenfunction  $\Phi$  cannot vanish to infinite order at  $(x, y)$ .*
- (ii) *If the non-zero eigenfunction  $\Phi$  vanishes at  $(x, y)$ , then the leading part of its Taylor expansion at  $(x, y)$  is a harmonic homogeneous polynomial.*

- (iii) If the point  $(x, y)$  is a critical zero of the eigenfunction  $\Phi$ , then the nodal set  $N(\Phi)$  at the point  $(x, y)$  consists of finitely many regular arcs which form an equi-angular system.
- (iv) The nodal set can only have self-intersections at critical zeroes, and the number of arcs which meet at a self-intersection is determined by the order of vanishing of the eigenfunction. Nodal curves cannot meet tangentially.
- (v) The nodal set cannot have an end point in the interior of  $\mathcal{S}$ , and consists of finitely many analytic arcs.
- (vi) Let the eigenfunction  $\Phi$  be associated with the eigenvalue  $\lambda$ . If  $\omega$  is a nodal domain, i.e., a connected component of  $\mathcal{S} \setminus N(\Phi)$ , then the first Dirichlet eigenvalue of  $\omega$  is equal to  $\lambda$ .
- (vii) Similar properties hold at boundary points, in particular property (iii).

**Remark.** Since the eigenfunctions of  $\mathcal{S}$  are defined over the whole plane, the analysis of the critical zeroes at interior points easily extends to the boundary.

**Properties 5.3** Let  $\Phi$  be an eigenfunction  $\Phi_{m,n}^\theta$  of the square  $\mathcal{S} = ]0, \pi[^2$ , with  $\theta \in [0, \pi[$ .

- (i) For  $\theta \neq \frac{\pi}{2}$ , the nodal set  $N(\Phi)$  satisfies

$$\mathcal{L} \cup \partial\mathcal{S} \subset N(\Phi) \subset \mathcal{L} \cup \partial\mathcal{S} \cup \{(x, y) \in [0, \pi]^2 \mid \cos \theta X(x, y) Y(x, y) < 0\}. \quad (5.7)$$

- (ii) If  $\gcd(m, n) = 1$ , then all the points in  $\mathcal{L}$  are regular points of the nodal set.
- (iii) The nodal set  $N(\Phi)$  can only hit the boundary of the square at critical zeroes (either in the interior of the edges or at the vertices).
- (iv) The nodal set  $N(\Phi)$  can only pass from one connected component of the set

$$\mathcal{W}_{m,n}^\theta := \{(x, y) \in [0, \pi]^2 \mid \cos \theta X(x, y) Y(x, y) < 0\}$$

to another through one of the points in  $\mathcal{L}$ .

- (v) No closed connected component of  $N(\Phi)$  can be contained in the closure of one of the connected components of  $\mathcal{W}_{m,n}^\theta$ . Equivalently, any connected component of  $N_i(\Phi)$  must contain at least one point in  $\mathcal{L}$ .

**Proof.** (i) We have  $\sin \theta > 0$ , so that for  $\cos \theta X(x, y) Y(x, y) \geq 0$  the function  $\Phi$  is either positive or negative, it cannot vanish unless  $(x, y) \in \mathcal{L}$ . (ii) Follows by direct analysis. (iii) Follows from Property 5.2. (iv) Clear. (v) Any connected component of  $N(\Phi)$  which does not meet  $\mathcal{L}$  would be strictly contained in one of the nodal domains of the eigenfunctions  $X$  or  $Y$ , a contradiction with Property 5.2 (vi).  $\square$

Figure 5.1 illustrates property (i) when  $(m, n) = (1, 3), (1, 4)$  or  $(2, 3)$ . When  $\cos \theta > 0$ , the nodal set is contained in the white sub-squares; when  $\cos \theta < 0$  it is contained in the grey sub-squares. The points in  $\mathcal{L}$  are the points labelled  $a, b, \dots$  in the figures.

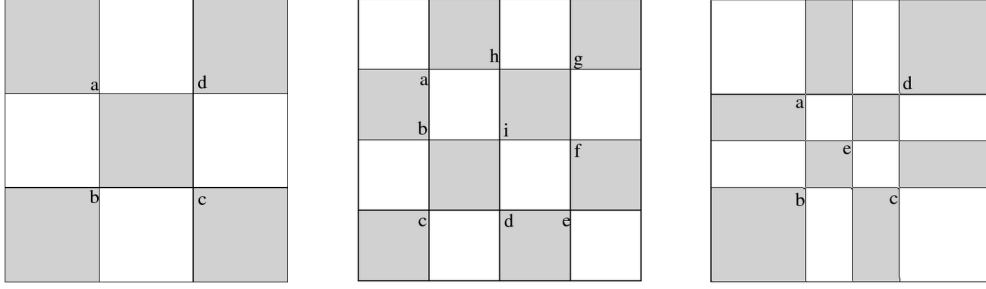


Figure 5.1: Checkerboards for eigenvalues  $\hat{\lambda}_{1,3}$ ,  $\hat{\lambda}_{1,4}$  and  $\hat{\lambda}_{2,3}$

### 5.3 Notation and definitions, II.

We now consider the case of the eigenvalue  $\hat{\lambda}_{1,R} = 1 + R^2$ , for some integer  $R \geq 1$ . We introduce

- the numbers

$$p_i := i \frac{\pi}{R}, \text{ for } 0 \leq i \leq R, \quad (5.8)$$

$$m_i := \left(i + \frac{1}{2}\right) \frac{\pi}{R}, \text{ for } 0 \leq i \leq R-1, \quad (5.9)$$

- the collection of squares

$$Q_{i,j} := ]p_i, p_{i+1}[ \times ]p_j, p_{j+1}[, \text{ for } 0 \leq i, j \leq R-1, \quad (5.10)$$

whose centers are the points  $(m_i, m_j)$ ,

- the lattice

$$\mathcal{L} := \{(p_i, p_j) \mid 1 \leq i, j \leq R-1\}. \quad (5.11)$$

**Coloring the squares.** Assume that  $\theta \neq 0$  and  $\frac{\pi}{2}$ . If  $(-1)^{i+j} \cos \theta < 0$ , we color the square  $Q_{i,j}$  in white, otherwise we color it in grey. The collection of squares  $\{Q_{i,j}\}$  becomes a grey/white checkerboard (which depends on  $R$  and on the sign of  $\cos \theta$ ). Depending on the sign of  $\cos \theta$ , the white part of the checkerboard is given by,

$$\begin{aligned} \mathcal{W}(+) &:= \bigcup_{(-1)^{i+j}=-1} Q_{i,j}, \text{ when } \cos \theta > 0, \\ \mathcal{W}(-) &:= \bigcup_{(-1)^{i+j}=1} Q_{i,j}, \text{ when } \cos \theta < 0. \end{aligned} \quad (5.12)$$

For the eigenfunction  $\Phi^\theta$ , we have,

$$\mathcal{L} \cup \partial \mathcal{S} \subset N(\Phi^\theta) \subset \mathcal{W}(\pm) \cup \mathcal{L} \cup \partial \mathcal{S}, \quad (5.13)$$

if  $(\pm \cos \theta > 0)$ .

**Remark.** Observe that the squares  $Q_{i,j}$  are open, the sets  $\mathcal{W}(\pm)$  do not contain the segments  $\{x = p_i\} \cap \mathcal{S}$  and  $\{y = p_j\} \cap \mathcal{S}$ .



Figure 5.2 shows the checkerboards for the eigenvalue  $\hat{\lambda}_{1,8}$ , when  $\cos \theta > 0$ , *resp.* for  $\hat{\lambda}_{1,9}$ , when  $\cos \theta < 0$ .

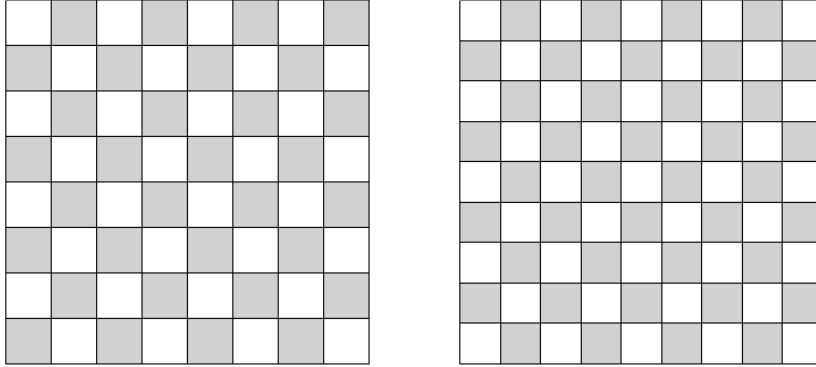


Figure 5.2: Checkerboards  $\mathcal{W}(+)$  for the eigenvalue  $\hat{\lambda}_{1,8}$ , and  $\mathcal{W}(-)$  for the eigenvalue  $\hat{\lambda}_{1,9}$

To describe the global aspect of the nodal sets, we will also use the following squares.

Denote by

$$r := \left[ \frac{R}{2} \right], \quad (5.14)$$

the integer part of  $R/2$ . For  $0 \leq i \leq r$ , define the square

$$\mathcal{S}_i := ]p_i, p_{R-i}[ \times ]p_i, p_{R-i}[. \quad (5.15)$$

With this notation, we have

$$\mathcal{S}_r \subset \mathcal{S}_{r-1} \subset \cdots \subset \mathcal{S}_0 = \mathcal{S}.$$

Furthermore, when  $R = 2r$ ,  $\mathcal{S}_{r-1} = ]p_{r-1}, p_{r+1}[^2$  consists of four  $Q$ -squares, while  $\mathcal{S}_r$  is empty; when  $R = 2r+1$ ,  $\mathcal{S}_r$  is a single  $Q$ -square. All these squares have the same center  $O = (\pi/2, \pi/2)$ .

## 6 Eigenfunctions associated with the eigenvalue $\hat{\lambda}_{1,R}$

In this section, we consider the eigenfunctions associated with the eigenvalue  $\hat{\lambda}_{1,R}$ , for an integer  $R \geq 1$ . More precisely, we consider the 1-parameter family of eigenfunctions,

$$\Phi^\theta(x, y) := \Phi(x, y, \theta) := \cos \theta \sin x \sin(Ry) + \sin \theta \sin(Rx) \sin y, \quad (6.1)$$

where  $x, y \in [0, \pi]^2$  and  $\theta \in [0, \pi[$ .

This eigenfunction can be written as

$$\Phi(x, y, \theta) = \sin x \sin y \phi(x, y, \theta), \quad (6.2)$$

with

$$\phi(x, y, \theta) := \cos \theta U_{R-1}(\cos y) + \sin \theta U_{R-1}(\cos x), \quad (6.3)$$

where  $U_n(t)$  is the  $n$ -th Chebyshev polynomial of second type defined by the relation,

$$\sin t U_n(\cos t) := \sin((n+1)t). \quad (6.4)$$

## 6.1 Chebyshev polynomials and special values of $\theta$

In this section, we list some properties of the Chebyshev polynomials to be used later on.

**Properties 6.1** For  $R \in \mathbb{N} \setminus \{0\}$ , the Chebyshev polynomial  $U_{R-1}(t)$  has the following properties.

- (i) The polynomial  $U_{R-1}$  has degree  $R-1$  and the same parity as  $R-1$ . Its zeroes are the points  $\cos p_j, 1 \leq j \leq R-1$ , see (5.8). Furthermore,  $U_{R-1}(1) = R$ ,  $U_{R-1}(-1) = (-1)^{R-1}R$ , and  $-R \leq U_{R-1}(t) \leq R$  for all  $t \in [-1, 1]$ .
- (ii) The polynomial  $U'_{R-1}$  has exactly  $R-2$  simple zeroes  $\cos q_j, 1 \leq j \leq R-2$ , with  $q_j \in ]p_j, p_{j+1}[$ .
- (iii) When  $R$  is even,  $R = 2r$ , the values  $q_j$  satisfy,

$$\begin{aligned} 0 < q_1 < q_2 < \dots < q_{r-1} < \frac{\pi}{2} < q_r < \dots < q_{2r-2} < \pi, \\ q_{2r-1-j} &= \pi - q_j, \quad 1 \leq j \leq r-1. \end{aligned} \quad (6.5)$$

- (iv) When  $R$  is odd,  $R = 2r + 1$ , the values  $q_j$  satisfy,

$$\begin{aligned} 0 < q_1 < q_2 < \dots < q_{r-1} < q_r = \frac{\pi}{2} < q_{r+1} < \dots < q_{2r-1} < \pi, \\ q_{2r-j} &= \pi - q_j, \quad 1 \leq j \leq r-1. \end{aligned} \quad (6.6)$$

- (v) Let  $M_j := U_{R-1}(\cos q_j)$ , for  $1 \leq j \leq R-2$ , denote the local extrema of  $U_{R-1}$ . Then,

$$\begin{aligned} (-1)^j M_j &> 0 \text{ and } (-1)^j U_{R-1}(\cos t) > 0 \text{ in } ]p_j, p_{j+1}[, \\ (-1)^{j+1} (U_{R-1}(\cos t) - M_j) &\geq 0 \text{ in } ]p_j, p_{j+1}[. \end{aligned} \quad (6.7)$$

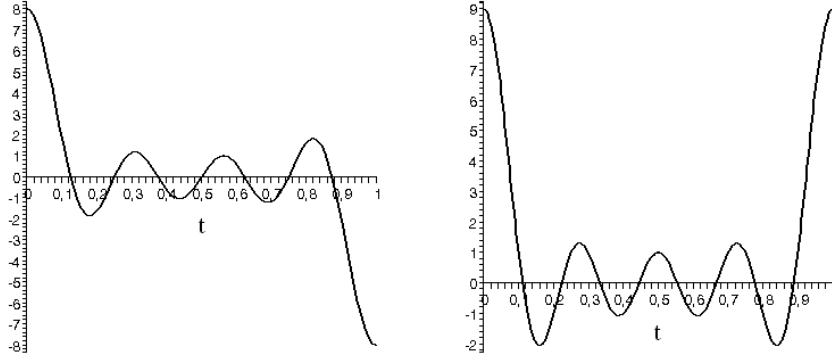


Figure 6.1: Functions  $U_7(\cos(\pi t))$  and  $U_8(\cos(\pi t))$

**Proof.** The above properties are easy to prove, and illustrated by the graph of the function  $t \rightarrow U_{R-1}(\cos t)$  in the interval  $[0, \pi]$ , see Figure 6.1, for the cases  $R = 8$  and  $R = 9$ .  $\square$

**Special values of the parameter  $\theta$ .** We shall now associate some special values of the parameter  $\theta$  with the zeroes

$$\mathcal{Q} := \{q_j \mid 1 \leq j \leq R-2\} \quad (6.8)$$

of the function  $t \rightarrow U'_{R-1}(\cos t)$ . As we shall see later on, they are related to changes in the nodal patterns of the eigenfunctions  $\Phi^\theta$  when  $\theta$  varies from 0 to  $\pi$ .

The values of  $\theta$  to be introduced below are well defined because the polynomial  $U_{R-1}$  does not vanish at the points  $\cos q_k$ ,  $1 \leq k \leq R-2$ . These values of  $\theta$  will clearly depend on  $R$ , although we do not indicate the dependence in the notations.

- For  $1 \leq i, j \leq R-2$ , define  $\theta(q_i, q_j)$ , alias  $\theta_{i,j}$ , to be the unique angle in the interval  $[0, \pi[$  such that

$$\cos \theta_{i,j} U_{R-1}(\cos q_j) + \sin \theta_{i,j} U_{R-1}(\cos q_i) = 0. \quad (6.9)$$

Let  $\mathcal{T}_o$  denote the corresponding set,

$$\mathcal{T}_o := \{\theta_{i,j} \mid 1 \leq i, j \leq R-2\}. \quad (6.10)$$

- For  $* \in \{0, \pi\}$ , and  $1 \leq j \leq R-2$ , define  $\theta(*, q_j)$ , alias  $\theta_{*,j}$ , to be the unique angle in the interval  $[0, \pi[$  such that

$$\cos \theta_{*,j} U_{R-1}(\cos q_j) + \sin \theta_{*,j} U_{R-1}(\cos *) = 0. \quad (6.11)$$

Let  $\mathcal{T}_x$  denote the corresponding set,

$$\mathcal{T}_x := \{\theta_{*,j} \mid * \in \{0, \pi\}, 1 \leq j \leq R-2\}. \quad (6.12)$$

- For  $1 \leq i \leq R-2$ , and  $* \in \{0, \pi\}$ , define  $\theta(q_i, *)$ , alias  $\theta_{i,*}$ , to be the unique angle in the interval  $[0, \pi[$  such that

$$\cos \theta_{i,*} U_{R-1}(\cos *) + \sin \theta_{i,*} U_{R-1}(\cos q_i) = 0. \quad (6.13)$$

Let  $\mathcal{T}_y$  denote the corresponding set,

$$\mathcal{T}_y := \{\theta_{i,*} \mid * \in \{0, \pi\}, 1 \leq i \leq R-2\}. \quad (6.14)$$

Observe the following relations between the above values of  $\theta$ ,

$$\theta(q_j, q_i) = \frac{\pi}{2} - \theta(q_i, q_j). \quad (6.15)$$

When  $R = 2r + 1$  is odd, we have

$$\begin{aligned} \theta(q_i, q_j) &= \theta(\pi - q_i, \pi - q_j) = \theta(\pi - q_i, q_j) = \theta(q_i, \pi - q_j), \\ \theta(0, q_j) &= \theta(\pi, q_j), \\ \theta(q_i, 0) &= \theta(q_i, \pi). \end{aligned} \quad (6.16)$$

When  $R = 2r$  is even, we have

$$\begin{aligned} \theta(q_i, q_j) &= \theta(\pi - q_i, \pi - q_j), \\ \theta(\pi - q_i, q_j) &= \pi - \theta(q_i, q_j), \\ \theta(q_i, \pi - q_j) &= \pi - \theta(q_i, q_j), \\ \theta(\pi, q_j) &= \pi - \theta(0, q_j), \\ \theta(q_i, \pi) &= \pi - \theta(q_i, 0). \end{aligned} \quad (6.17)$$

Finally, define the number  $\theta_-$  to be,

$$\theta_- := \arctan\left(\frac{1}{R} \left| \inf_{[-1,1]} U_{R-1} \right| \right). \quad (6.18)$$

We have  $0 < \theta_- \leq \pi/4$ , with  $\theta_- = \pi/4$  when  $R$  is even, and  $\theta_- < \pi/4$  when  $R$  is odd.

**Remark.** The pictures and numerical computations seem to indicate that the infimum is achieved at  $\cos q_1$ .

**Examples.** Numerical computations give the following approximate data when  $R = 8$  or  $R = 9$ . The indication  $\pi$  after the set means that the values in the set should be multiplied by  $\pi$ .

- Special values of  $\theta$  when  $R = 8$ .

$$\begin{aligned} \mathcal{Q} &= \{0.179749, 0.309108, 0.436495, 0.563505, 0.690892, 0.820251\} \pi, \\ \mathcal{T}_o &= \{0.161605, 0.185335, 0.223323, 0.25, 0.276677, 0.314665, 0.338395, \\ &\quad 0.661605, 0.685335, 0.723323, 0.75, 0.776677, 0.814665, 0.838395\} \pi, \\ \mathcal{T}_x &= \{0.040363, 0.047665, 0.071705, 0.928295, 0.952335, 0.959636\} \pi, \\ \mathcal{T}_y &= \{0.428295, 0.452335, 0.459636, 0.540363, 0.547665, 0.571705\} \pi. \end{aligned} \quad (6.19)$$

- Special values of  $\theta$  when  $R = 9$ .

$$\begin{aligned} \mathcal{Q} &= \{0.159593, 0.274419, 0.387439, 0.500000, 0.612561, 0.725581, 0.840407\} \pi, \\ \mathcal{T}_o &= \{0.145132, 0.181901, 0.217145, 0.239975, 0.260025, 0.282855, \\ &\quad 0.318099, 0.354868, 0.653215, 0.707395, 0.75, 0.792605, 0.846785\} \pi, \\ \mathcal{T}_x &= \{0.037494, 0.070922, 0.953949, 0.964777\} \pi, \\ \mathcal{T}_y &= \{0.429078, 0.462505, 0.535223, 0.546050\} \pi. \end{aligned} \quad (6.20)$$

Up to symmetries, one can actually reduce the range of the parameter  $\theta$  to  $[0, \pi/4]$  when  $R$  is even, and to  $[\pi/4, 3\pi/4]$  when  $R$  is odd, see Subsection 6.2. Up to this reduction, the above values correspond to the values which appear in the figures showing the nodal patterns for the eigenvalues  $\hat{\lambda}_{1,8}$  and  $\hat{\lambda}_{1,9}$ , see Figures 6.9, 6.10, and 6.11 at the end of the paper).

## 6.2 Symmetries of the eigenfunctions associated with $\hat{\lambda}_{1,R}$

When studying the family of eigenfunctions  $\{\Phi^\theta\}$  associated with the eigenvalue  $\hat{\lambda}_{1,R}$ , it is useful to take symmetries into account.

**Properties 6.2** *The following relations hold for any  $(x, y) \in [0, \pi] \times [0, \pi]$  and  $\theta \in [0, \pi[$ .*

- (i) *For any  $R \in \mathbb{N} \setminus \{0\}$ ,*

$$\Phi(\pi - x, \pi - y, \theta) = (-1)^{R+1} \Phi(x, y, \theta). \quad (6.21)$$

*This relation implies that the nodal set  $N(\Phi^\theta)$  is symmetrical with respect to the center  $O$  of the square  $\mathcal{S}$ . Furthermore,*

$$\Phi(x, y, \frac{\pi}{2} - \theta) = \Phi(y, x, \theta). \quad (6.22)$$

(ii) When  $R$  is odd, the function  $\Phi$  has more symmetries, namely,

$$\Phi(\pi - x, y, \theta) = \Phi(x, \pi - y, \theta) = \Phi(x, y, \theta). \quad (6.23)$$

This means that the nodal set  $N(\Phi^\theta)$  is symmetrical with respect to the lines  $\{x = \pi/2\}$  and  $\{y = \pi/2\}$ .

(iii) When  $R$  is even, we have

$$\Phi(x, \pi - y, \theta) = \Phi(x, y, \pi - \theta) = -\Phi(\pi - x, y, \theta). \quad (6.24)$$

(iv) Up to symmetries with respect to the first diagonal, or to the lines  $\{x = \pi/2\}$  and  $\{y = \pi/2\}$ , the nodal patterns of the family of eigenfunctions  $\{\Phi^\theta\}$ , are those displayed by the sub-families  $\theta \in [0, \pi/4]$  when  $R$  is even, and  $\theta \in [\pi/4, 3\pi/4]$  when  $R$  is odd.

### 6.3 Critical zeroes of the eigenfunctions associated with $\hat{\lambda}_{1,R}$

Recall that a *critical zero* of the eigenfunction  $\Phi^\theta$  is a point  $(x, y) \in \bar{\mathcal{S}}$  such that

$$\Phi(x, y, \theta) = \Phi_x(x, y, \theta) = \Phi_y(x, y, \theta) = 0. \quad (6.25)$$

At a critical zero, the nodal set  $N(\Phi^\theta)$  consists of several arcs (or semi-arcs when the point is on  $\partial\mathcal{S}$ ) which form an equi-angular system, see Properties 5.2. Away from the critical zeroes, the nodal set consists of smooth embedded arcs. To determine the possible critical zeroes of  $\Phi^\theta$  is the key to describing the global aspect of the nodal set  $N(\Phi^\theta)$ .

We classify the critical zeroes into three (possibly empty) categories : (i) the *vertices* of the square  $\mathcal{S}$ ; (ii) the *edge critical zeroes* located in the interior of the edges, typically a point of the form  $(0, y)$ , with  $y \in ]0, \pi[$ ; (iii) the *interior critical zeroes* of the form  $(x, y) \in \mathcal{S}$ .

#### 6.3.1 Behaviour at the vertices

Using the symmetry of  $N(\Phi)$  with respect to the point  $O$ , see (6.21), it suffices to consider the vertices  $(0, 0)$  and  $(0, \pi)$ . Recalling (6.1) and (6.2), the Taylor expansion at  $(0, 0)$  of  $\phi(x, y, \theta)$  is given by,

$$\begin{aligned} \phi(x, y, \theta) = & R(\cos \theta + \sin \theta) \\ & + \frac{R(1 - R^2)}{6} (\cos \theta y^2 + \sin \theta x^2) \\ & + O(x^4 + y^4). \end{aligned} \quad (6.26)$$

When  $R$  is odd, the behaviour is the same at the four vertices and given by (6.26), due to the symmetries (6.23).

When  $R$  is even, the Taylor expansion of  $\phi(x, y, \theta)$  at  $(0, \pi)$ , follows from the previous one and relation (6.24). In the variables  $x$  and  $z$  such that  $y = \pi - z$ , we have,

$$\begin{aligned} \phi(x, \pi - z, \theta) = & R(-\cos \theta + \sin \theta) \\ & - \frac{R(1 - R^2)}{6} (-\cos \theta z^2 + \sin \theta x^2) \\ & + O(x^4 + z^4). \end{aligned} \quad (6.27)$$

With the link between  $\Phi$  and  $\phi$  in mind, we obtain:

**Properties 6.3** *The vertices of the square  $S$  are critical zeroes for the eigenfunction  $\Phi^\theta$  for all  $\theta$ .*

- (i) **Case  $R$  even.** *The vertices  $(0, \pi)$  and  $(\pi, 0)$  are non degenerate critical zeroes of  $\Phi^\theta$  if and only if  $\theta \neq \pi/4$ . When  $\theta = \pi/4$ , they are degenerate critical zeroes of order 4. The vertices  $(0, 0)$  and  $(\pi, \pi)$  are non-degenerate critical zeroes of  $\Phi$  if and only if  $\theta \neq 3\pi/4$ . When  $\theta = 3\pi/4$ , they are degenerate critical zeroes of order 4. The nodal patterns at the vertices are shown in Figure 6.2.*
- (ii) **Case  $R$  odd.** *The four vertices are non-degenerate critical zeroes of  $\Phi^\theta$  if and only if  $\theta \neq 3\pi/4$ . When  $\theta = 3\pi/4$ , they are degenerate critical zeroes of order 4. The nodal patterns at the vertices are shown in Figure 6.3.*

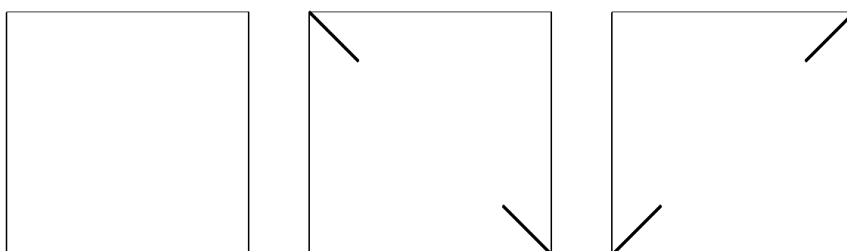


Figure 6.2:  $R$  even, nodal patterns at the vertices. From left to right,  $\theta \neq \pi/4$  and  $3\pi/4$  ;  $\theta = \pi/4$  ;  $\theta = 3\pi/4$

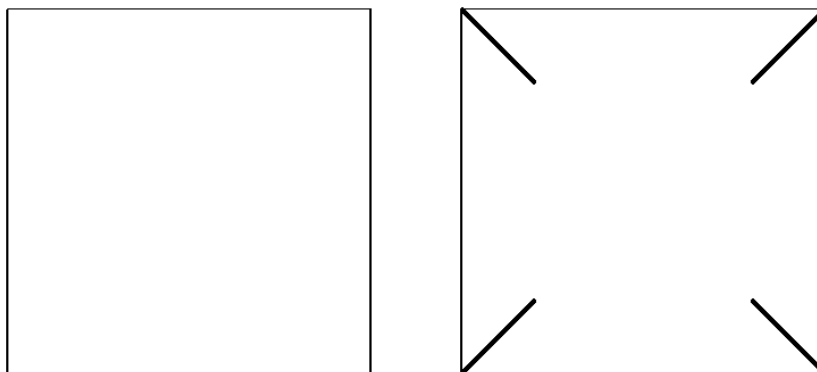


Figure 6.3:  $R$  odd, nodal patterns at the vertices. From left to right,  $\theta \neq 3\pi/4$  ;  $\theta = 3\pi/4$

### 6.3.2 Critical zeroes, formulas

To determine the critical zeroes of the eigenfunction  $\Phi$ , we recall our notation at the beginning of the section. The first partial derivatives with respect to  $x$  and  $y$  are given by,

$$\begin{aligned}\Phi_x(x, y, \theta) &= \cos x \sin y \phi(x, y, \theta) \\ &\quad - \sin \theta \sin^2 x \sin y U'_{R-1}(\cos x), \\ \Phi_y(x, y, \theta) &= \sin x \cos y \phi(x, y, \theta) \\ &\quad - \cos \theta \sin x \sin^2 y U'_{R-1}(\cos y).\end{aligned}\tag{6.28}$$

The second partial derivatives are given by,

$$\begin{aligned}\Phi_{xx}(x, y, \theta) &= -\sin x \sin y \phi(x, y, \theta) \\ &\quad - 3 \sin \theta \cos x \sin x \sin y U'_{R-1}(\cos x) \\ &\quad + \sin \theta \sin^3 x \sin y U''_{R-1}(\cos x), \\ \Phi_{xy}(x, y, \theta) &= \cos x \cos y \phi(x, y, \theta) \\ &\quad - \cos \theta \cos x \sin^2 y U'_{R-1}(\cos y) \\ &\quad - \sin \theta \sin^2 x \cos y U'_{R-1}(\cos x), \\ \Phi_{yy}(x, y, \theta) &= -\sin x \sin y \phi(x, y, \theta) \\ &\quad - 3 \cos \theta \sin x \cos y \sin y U'_{R-1}(\cos y) \\ &\quad + \cos \theta \sin x \sin^3 y U''_{R-1}(\cos y).\end{aligned}\tag{6.29}$$

### 6.3.3 Behaviour along the edges

Recall the notation of Subsection 6.1. Due (6.21), the symmetry with respect to the center  $O$  of the square  $\mathcal{S}$ , it suffices to consider the open edges  $\{0\} \times ]0, \pi[$  and  $]0, \pi[ \times \{0\}$ .

• **Critical zeroes on the edge  $\{0\} \times ]0, \pi[$ .** Using formulas (6.28) and (6.29), as well as Properties 6.1, we infer that the point  $(0, y)$  is a critical zero for  $\Phi^\theta$  if and only if,

$$\cos \theta U_{R-1}(\cos y) + R \sin \theta = 0,\tag{6.30}$$

with second derivatives at  $(0, y)$ ,  $\Phi_{xx} = \Phi_{yy} = 0$ , and  $\Phi_{xy} = -\cos \theta \sin^2 y U'_{R-1}(\cos y)$ .

The point  $(0, y)$  is a non degenerate critical zero, unless  $y = q_j \in \mathcal{Q}$  for some  $j, 1 \leq j \leq R-2$ . This can only occur when  $\theta = \theta(0, q_j)$ . In this case, the third derivative  $\Phi_{xy^2}$  at the degenerate critical zero  $(0, q_j)$  is equal to

$$\cos(\theta(0, q_j)) \sin^3 q_j U''_{R-1}(\cos q_j) \neq 0,$$

and the critical zero has order 3.

• **Critical zeroes on the edge  $]0, \pi[ \times \{0\}$ .** Similarly, the point  $(x, 0)$  is a critical zero for  $\Phi^\theta$  if and only if,

$$R \cos \theta + \sin \theta U_{R-1}(\cos x) = 0,\tag{6.31}$$

with second derivatives at  $(x, 0)$ ,  $\Phi_{xx} = \Phi_{yy} = 0$ , and

$$\Phi_{xy} = -\sin \theta \sin^2 x U'_{R-1}(\cos x).$$

The point  $(x, 0)$  is a non degenerate critical zero unless  $x = q_i \in \mathcal{Q}$  for some  $i, 1 \leq i \leq R - 2$ . This can only occur when  $\theta = \theta(q_i, 0)$ . In this case, the third derivative  $\Phi_{x^2y}$  at the degenerate critical zero  $(q_i, 0)$  is equal to

$$\sin(\theta(q_i, 0)) \sin^3 q_i U''_{R-1}(\cos q_i) \neq 0,$$

and the critical zero has order 3.

**Remark.** At an edge critical zero which is non degenerate, an arc from the nodal set hits the edge orthogonally. At a degenerate edge critical zero, two arcs from the nodal set hit the edge with equal angle  $\pi/3$ . See Figures 6.5 and 6.6.

The following properties summarize the analysis of the above equations.

**Properties 6.4** *The critical zeroes on the open edges, if any, appear in pairs of points which are symmetrical with respect to the center  $O$  of the square  $\mathcal{S}$ .*

**Case  $R$  even.**

- (i) *For  $\theta \in [0, \pi/4[ \cup ]3\pi/4, \pi[$ , there are critical zeroes on the vertical edges  $\{0, \pi\} \times ]0, \pi[$ , and no critical zero on the horizontal edges  $]0, \pi[ \times \{0, \pi\}$ .*
- (ii) *For  $\theta \in ]\pi/4, 3\pi/4[$ , there are critical zeroes on the horizontal edges  $]0, \pi[ \times \{0, \pi\}$ , and no critical zero on the vertical edges  $\{0, \pi\} \times ]0, \pi[$ .*
- (iii) *The number of critical zeroes depends on  $\theta$ , more precisely on the number of solutions of (6.30) or (6.31).*
- (iv) *When  $\theta = \pi/4$  or  $3\pi/4$ , the only boundary critical zeroes are vertices, see Properties 6.3.*

**Case  $R$  odd.**

- (i) *Recall the value  $0 < \theta_- < \pi/4$  defined in Subsection 6.1. For  $\theta \in [0, \theta_-] \cup ]3\pi/4, \pi[$ , there are critical zeroes on the vertical edges  $\{0, \pi\} \times ]0, \pi[$ , and no critical zero on the horizontal edges  $]0, \pi[ \times \{0, \pi\}$ .*
- (ii) *For  $\theta \in [\pi/2 - \theta_-, 3\pi/4[$ , there are critical zeroes on the horizontal edges  $]0, \pi[ \times \{0, \pi\}$ , and no critical zero on the vertical edges  $\{0, \pi\} \times ]0, \pi[$ .*
- (iii) *For  $\theta \in ]\theta_-, \pi/2 - \theta_-[$ , there is no critical zero on the open edges.*
- (iv) *The number of critical zeroes depends on  $\theta$ , more precisely on the number of solutions of (6.30) or (6.31).*
- (v) *The critical zeroes have order at most 3. Degenerate critical zeroes can only occur for finitely many values of  $\theta$  and  $x$  or  $y$ .*
- (vi) *When  $\theta = 3\pi/4$ , the only boundary critical zeroes are the vertices, see Properties 6.3.*

*In both cases, the edge critical zeroes are non degenerate unless they occur on a horizontal edge for some  $x = q_i \in \mathcal{Q}$ , resp. on a vertical edge for some  $y = q_j \in \mathcal{Q}$ , in which case  $\theta$  must be equal to  $\theta(q_i, 0)$ , resp. to  $\theta(0, q_j)$ . Degenerate critical zeroes have order 3. If  $\theta \neq 0$  or  $\pi/2$ , the points  $(*, p_j)$  and  $(p_j, *)$  with  $1 \leq j \leq R - 1$  and  $* = 0$  or  $\pi$  are not critical zeroes of the eigenfunction  $\Phi^\theta$ .*

**Remark.** A more detailed description of the localization of the edge critical zeroes is given in Subsection 6.4.



### 6.3.4 Interior critical zeroes

Recall the notations of Subsection 6.1. The following properties follow from (6.28)–(6.29).

**Properties 6.5** *Let  $(x, y) \in \mathcal{S}$  be an interior point.*

(i) *The functions  $\Phi$  and  $\Phi_x$  vanish at  $(x, y)$  if and only if*

$$\begin{aligned} \cos \theta U_{R-1}(\cos y) + \sin \theta U_{R-1}(\cos x) &= 0, \text{ and} \\ U'_{R-1}(\cos x) &= 0. \end{aligned} \tag{6.32}$$

*This happens in particular at regular points of the nodal set with a horizontal tangent.*

(ii) *The functions  $\Phi$  and  $\Phi_y$  vanish at  $(x, y)$  if and only if*

$$\begin{aligned} \cos \theta U_{R-1}(\cos y) + \sin \theta U_{R-1}(\cos x) &= 0, \text{ and} \\ U'_{R-1}(\cos y) &= 0. \end{aligned} \tag{6.33}$$

*This happens in particular at regular points of the nodal set with a vertical tangent.*

(iii) *The point  $(x, y)$  is an interior critical zero of  $\Phi$ , if and only if*

$$\begin{aligned} \cos \theta U_{R-1}(\cos y) + \sin \theta U_{R-1}(\cos x) &= 0, \text{ and} \\ U'_{R-1}(\cos x) = 0 \text{ and } U'_{R-1}(\cos y) &= 0. \end{aligned} \tag{6.34}$$

*The only possible interior critical zeroes for the family of eigenfunctions  $\{\Phi^\theta\}$  are the points  $(q_i, q_j)$ ,  $1 \leq i, j \leq R-2$ . The point  $(q_i, q_j)$  can only occur as a critical zero of the eigenfunction  $\Phi^{\theta(q_i, q_j)}$ . When  $\theta$  is not one of the values  $\theta(q_i, q_j)$ ,  $1 \leq i, j \leq R-2$ , the eigenfunction  $\Phi^\theta$  does not have any interior critical zero.*

(iv) *When  $(x, y)$  is an interior critical zero of  $\Phi$ , the Hessian of  $\Phi$  at  $(x, y)$  is given by,*

$$\sin x \sin y \begin{pmatrix} \sin \theta \sin^2 x U''_{R-1}(\cos x) & 0 \\ 0 & \cos \theta \sin^2 y U''_{R-1}(\cos y) \end{pmatrix},$$

*so that the interior critical zeroes, if any, are always non degenerate.*

(v) *The lattice points  $\mathcal{L} = \{(\frac{i\pi}{R}, \frac{j\pi}{R}), 1 \leq i, j \leq R-1\}$  (see Subsection 5.3) are common zeroes to all the eigenfunctions  $\Phi^\theta$  when  $\theta \in [0, \pi[$ . They are not interior critical zeroes.*

## 6.4 $Q$ -nodal patterns of eigenfunctions associated with $\hat{\lambda}_{1,R}$

The purpose of this section is to list all the possible patterns of the nodal set  $N(\Phi^\theta)$  inside the  $Q$ -squares  $Q_{i,j}$ ,  $0 \leq i, j \leq R-1$ , see Subsection 5.3.

The following properties are derived from the previous sections and from Properties 5.3.

- (i) The nodal set  $N(\Phi^\theta)$  is contained in  $\mathcal{W}(\pm) \cup \mathcal{L} \cup \partial\mathcal{S}$ .
- (ii) If a white square  $Q_{i,j}$  does not touch the boundary  $\partial\mathcal{S}$ , the nodal set  $N(\Phi^\theta)$  cannot cross nor hit the boundary of  $Q_{i,j}$ , except at the vertices which belong to  $\mathcal{L}$ .
- (iii) If a white square  $Q_{i,j}$  touches the boundary  $\partial\mathcal{S}$ , the nodal set  $N(\Phi^\theta)$  cannot intersect the boundary of  $Q_{i,j}$ , except at the vertices which belong to  $\mathcal{L}$ , or at an edge contained in  $\partial\mathcal{S}$ .

- (iv) Since the points in  $\mathcal{L}$  are not critical zeroes, the nodal set consists of a single regular arc at such a point.
- (v) Inside a white square  $Q_{i,j}$ , the nodal set  $N(\Phi^\theta)$  can have at most one self intersection at  $(q_i, q_j)$  if this point is a critical zero for  $\Phi^\theta$ . In this case, the critical zero is non degenerate, and the nodal set at  $(q_i, q_j)$  consists locally of two regular arcs meeting orthogonally.
- (vi) Inside a square  $Q_{i,j}$ , the nodal set cannot stop at a point, and consists of at most finitely many arcs.
- (vii) The nodal set  $N(\Phi^\theta)$  cannot contain a closed curve contained in the closure of  $Q_{i,j}$  (energy reasons).

• **Inner  $Q$ -square.** Figure 6.4 shows all the possible nodal patterns inside a square  $Q_{i,j}$  which does not touch the boundary. The patterns A and B occur when the eigenfunction  $\Phi^\theta$  does not have any interior critical zero inside the  $Q$ -square. Pattern C occurs when  $\Phi^\theta$  admits  $(q_i, q_j)$  as interior critical zero (necessarily unique and non degenerate), in which case  $\theta$  must be equal to  $\theta(q_i, q_j)$ . The properties recalled above show that there are no other possible nodal patterns.

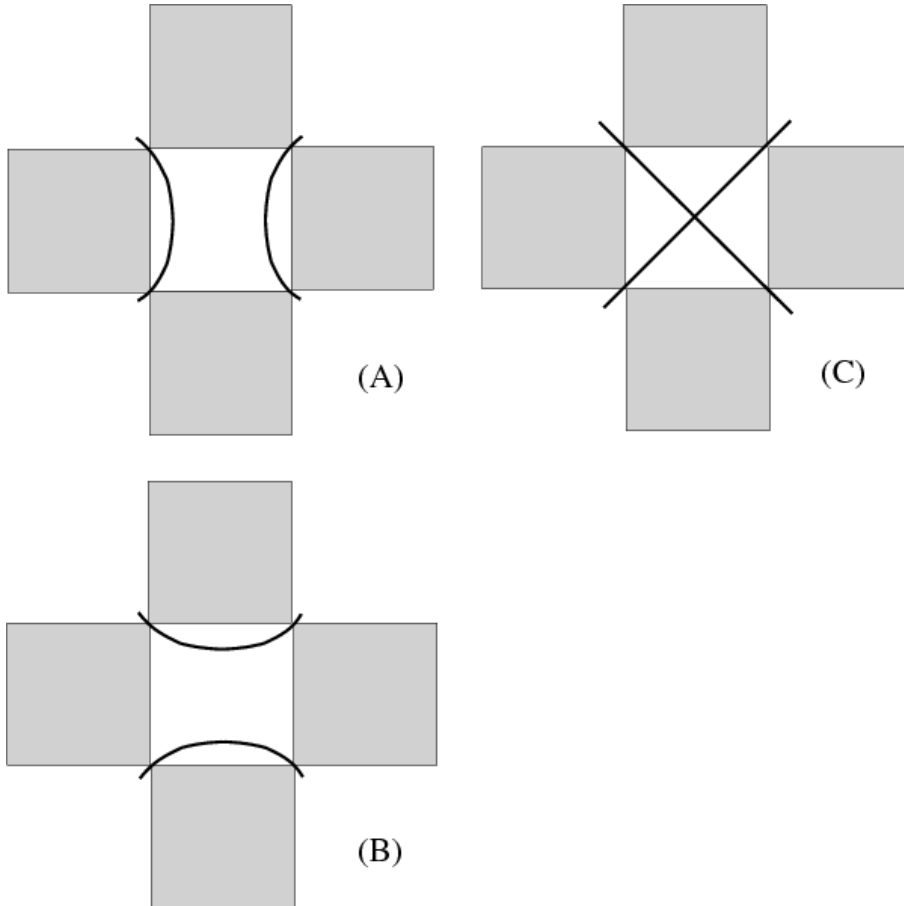


Figure 6.4: Nodal pattern in an inner  $Q$ -square

• **Boundary  $Q$ -square,  $R$  even.** As stated in Properties 6.2 (iv), it suffices to consider the case  $\theta \in [0, \pi/4]$ . The only boundary critical zeroes of  $\Phi^\theta$  are the vertices  $(0, \pi)$  and  $(\pi, 0)$ , this

case occurs if and only if  $\theta = \pi/4$ , and points on the vertical edges  $\{0, \pi\} \times ]0, \pi[$  if and only if  $0 \leq \theta < \pi/4$ . These points come in pairs of symmetric points with respect to the center  $O$  of the square  $\mathcal{S}$ . It suffices to describe the points located on the edge  $\{0\} \times ]0, \pi[$ , i.e., the points  $(0, y)$  satisfying equation (6.30),

$$U_{R-1}(\cos y) + R \tan \theta = 0, \text{ for some } \theta, \quad 0 \leq \theta < \pi/4.$$

When  $\theta = 0$ , this equation provides exactly  $(R - 1)$  non degenerate critical zeroes, the points  $p_j, 1 \leq j \leq R - 1$ . When  $0 < \theta < \pi/4$  the equation has at least one solution located in the interval  $]p_{R-1}, \pi[$ . This is the sole solution when  $\theta$  is close enough to  $\pi/4$ , and it corresponds to a non degenerate critical zero. The other solutions, if any, are located in the intervals  $]p_j, p_{j+1}[$ , with  $j$  odd. Each such interval contains at most two solutions, which correspond to non degenerate critical zeroes. When an interval contains only one point, this is a double solution, and it corresponds to a degenerate critical zero  $q_j$ . This can only occur for the special value  $\theta(0, q_j)$ .

Figure 6.5 gives all the possible nodal patterns of the eigenfunction  $\Phi^\theta$  in a square  $Q_{0,j}$  which touches the edge  $\{0\} \times ]0, \pi[$ . The base point of the square  $(0, p_j)$  is the black dot in the figures. The other dot is the vertex  $(0, \pi)$ .

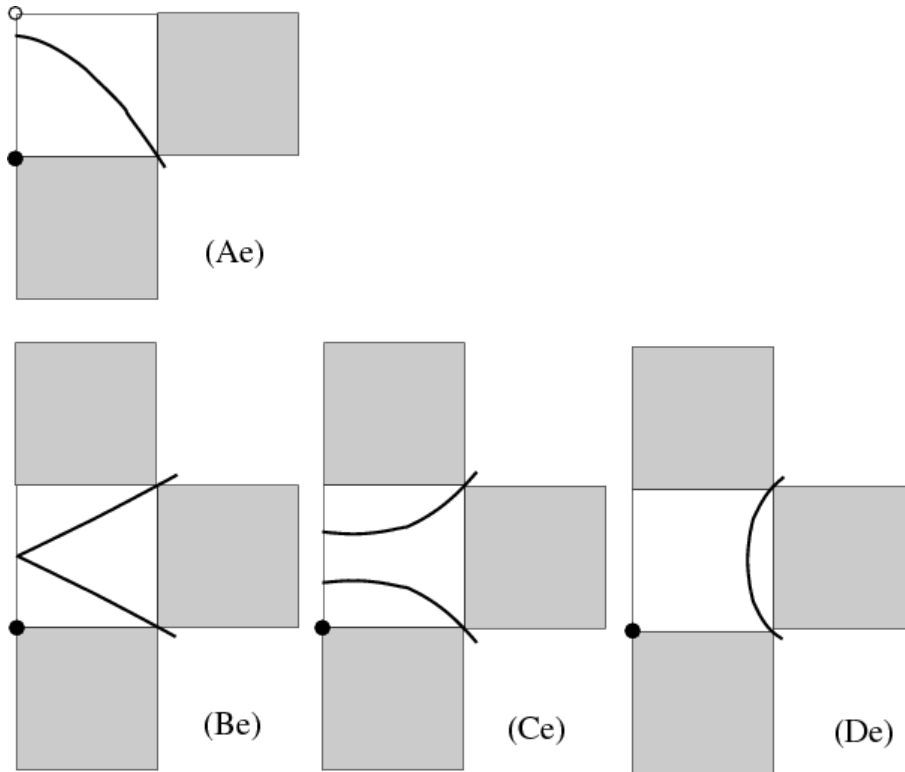


Figure 6.5: Local nodal patterns at the boundary,  $R$  even

Figure (Ae) shows the nodal pattern in the square  $Q_{0,R-1}$  which touches the vertex  $(0, \pi)$ , and contains the persistent edge non degenerate critical zero. Figure (Be) shows the nodal pattern when there is a degenerate edge critical zero  $(0, q_j)$ ; it is always of order three, with two arcs hitting the boundary with equal angles  $\pi/3$ . Figure (Ce) shows the nodal pattern when there are two non degenerate critical zeroes in the interval  $\{0\} \times ]p_j, p_{j+1}[$ . There are two arcs hitting the

boundary orthogonally. Figure (De) shows the nodal pattern when the interval  $\{0\} \times ]p_j, p_{j+1}[$  contains no critical zero. The properties recalled above show that there are no other possible nodal patterns.

• **Boundary  $Q$ -square,  $R$  odd.** The description of the critical zeroes of  $\Phi^\theta$  on the boundary  $\partial\mathcal{S}$  in the case  $R$  odd is similar to the case  $R$  even, with some changes. As stated in Properties 6.2 (iv), up to symmetries, we can restrict ourselves to  $\theta \in [\pi/4, 3\pi/4]$ . Recall the value  $0 < \theta_- < \pi/4$  defined in Subsection 6.1. The vertices are critical zeroes, and they are non degenerate unless  $\theta = 3\pi/4$ . For  $\theta \in [\pi/4, \pi/2 - \theta_-[$ , there is no critical zero on the edges. For  $\theta \in ]\pi/2 - \theta_-, 3\pi/4[$ , there are critical zeroes on the horizontal edges, and none on the vertical edges. Since the nodal sets are symmetrical with respect to  $\{y = \pi/2\}$ , it suffices to describe the critical zeroes on the horizontal edge  $]0, \pi[\times\{0\}$ . For  $\theta = \pi/2 - \theta_-$ , there are at least two order 3 critical zeroes (except when  $R = 3$  in which case there is only one). As a matter of fact, it seems that there are exactly two critical zeroes for  $R \geq 5$  because the local extrema of  $U_{R-1}$  decrease in absolute value on  $[-1, 0]$ . For  $\theta \in ]\pi/2 - \theta_-, \pi/2]$ , the number of critical zeroes depends on the number of solutions of equation (6.31),

$$R \cot \theta + U_{R-1}(\cos x) = 0,$$

with 0 or 2 solutions in each interval  $]p_i, p_{i+1}[\times\{0\}$ , or a degenerate critical zero at some  $(q_i, 0)$ , when  $\theta = \theta(q_i, 0)$ . For  $\theta \in ]\pi/2, 3\pi/4[$ , there are two non degenerate critical zeroes, one in each interval  $]0, p_1[\times\{0\}$  and  $]p_{R-1}, \pi[\times\{0\}$ , near the vertices. For  $\theta = 3\pi/4$ , there is no critical zero on the open edge, and only critical zeroes of order 4 at the vertices. Using the properties listed at the beginning of Subsection 6.4, one can show that Figure 6.6 contains all the possible nodal patterns in a  $Q$ -square touching the edge  $]0, \pi[\times\{0\}$ .

## 6.5 Nodal sets of the functions $Z_\pm$ associated with $\hat{\lambda}_{1,R}$

Recall the notation in Subsection 5.3, (5.15),  $Z_+ = \Phi^{\frac{\pi}{4}}$  and  $Z_- = \Phi^{\frac{3\pi}{4}}$ . The purpose of this section is to prove the following proposition.

**Proposition 6.6** *Nodal sets of the eigenfunctions  $Z_\pm$  associated with the eigenvalue  $\hat{\lambda}_{1,R}$ .*

- (i) **Case  $R$  even,  $R = 2r$ .** *The symmetries with respect to the lines  $\{x = \pi/2\}$  and  $\{y = \pi/2\}$  send the nodal set  $N(Z_+)$  to the nodal set  $N(Z_-)$ . Both nodal sets  $N(Z_+)$  and  $N(Z_-)$  are invariant under the symmetry with respect to the center  $O$  of the square. The nodal set  $N(Z_+)$  consists of the boundary  $\partial\mathcal{S}$ , the anti-diagonal, and a collection of  $(r - 1)$  simple closed curves  $\gamma_i$ . The curve  $\gamma_i$  winds around  $\partial\mathcal{S}_i$ , passing through the points in  $\mathcal{L} \cap \partial\mathcal{S}_i$ , and crosses the anti-diagonal  $\mathcal{D}_-$  orthogonally. The curves  $\gamma_i$  do not intersect each other.*
- (ii) **Case  $R$  odd,  $R = 2r + 1$ .** *The nodal sets  $N(Z_\pm)$  are invariant under the symmetries with respect to the lines  $\{x = \pi/2\}$  and  $\{y = \pi/2\}$ . The nodal set  $N(Z_+)$  consists of the boundary  $\partial\mathcal{S}$ , and a collection of  $r$  simple closed curves  $\alpha_i$ . The curve  $\alpha_i$  winds around  $\partial\mathcal{S}_i$ , passing through the points in  $\mathcal{L} \cap \partial\mathcal{S}_i$ . The curves  $\alpha_i$  do not intersect each other. The nodal set  $N(Z_-)$  consists of the boundary  $\partial\mathcal{S}$ , the two diagonals  $\mathcal{D}_\pm$ , and a collection of  $(r - 1)$  simple closed curves  $\beta_i$ . The curve  $\beta_i$  winds around  $\partial\mathcal{S}_i$ , passing through the points in  $\mathcal{L} \cap \partial\mathcal{S}_i$ , and crosses the diagonals  $\mathcal{D}_\pm$  orthogonally. The curves  $\beta_i$  do not intersect each other.*

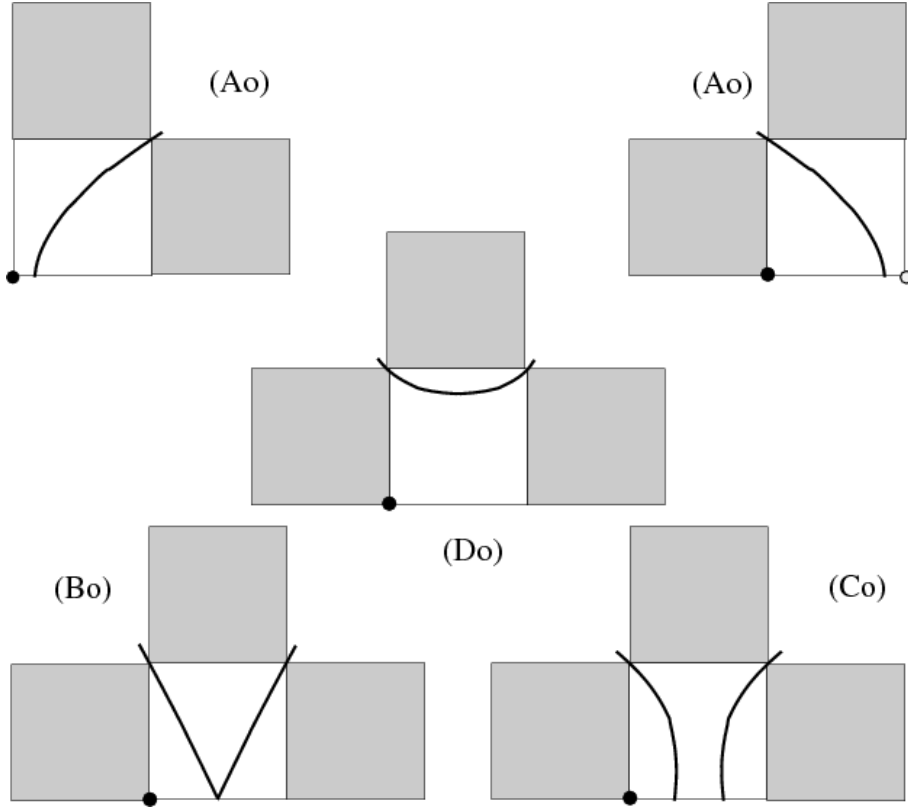


Figure 6.6: Local nodal patterns at the boundary,  $R$  odd

The proof of this proposition relies on three lemmas which we prove below. Lemma 6.7 determines precisely the interior critical zeroes of the nodal sets  $N(Z_{\pm})$ . Lemma 6.8 and 6.9 are “separation” lemmas.

**Lemma 6.7** *When  $R$  is even, the diagonal, resp. the anti-diagonal, is contained in the nodal set  $N(Z_-)$ , resp. in the nodal set  $N(Z_+)$ . When  $R$  is odd, the diagonal and anti-diagonal meet the nodal set  $N(Z_+)$  at finitely many points. They are both contained in the nodal set  $N(Z_-)$ . The critical zeroes of the functions  $Z_{\pm}$  are as follows.*

- (i) **Case  $R$  even**,  $R = 2r$ . *The interior critical zeroes of the function  $Z_+$  are exactly the  $(R - 2)$  points,  $(q_i, \pi - q_i)$ , for  $1 \leq i \leq R - 2$ , located on the anti-diagonal. The interior critical zeroes of the function  $Z_-$  are precisely the  $(R - 2)$  points,  $(q_i, q_i)$ , for  $1 \leq i \leq R - 2$ , located on the diagonal.*
- (ii) **Case  $R$  odd**,  $R = 2r + 1$ . *The function  $Z_+$  has no interior critical zero. The interior critical zeroes of the function  $Z_-$  are precisely the  $(2R - 5)$  points,  $(q_i, q_i)$ ,  $(q_i, \pi - q_i)$ , for  $1 \leq i \leq R - 2$ , located on the diagonal and anti-diagonal.*

**Remark.** Note that Lemma 6.7, Properties 6.4 and Properties 6.3 provide a complete description of the critical zeroes of the functions  $Z_{\pm}$ .

**Proof.** The first assertions are clear. We concentrate on the determination of the interior critical zeroes. Let  $\epsilon = \pm 1$ . The point  $(x, y) \in \mathcal{S}$  is a critical zero of the function  $Z_{\pm}$  if and only

if  $(x, y)$  is a common solution to the following three equations.

$$\sin x \sin(Ry) + \epsilon \sin(Rx) \sin y = 0. \quad (6.35)$$

$$\cos x \sin(Ry) + \epsilon R \cos(Rx) \sin y = 0. \quad (6.36)$$

$$R \sin x \cos(Ry) + \epsilon \sin(Rx) \cos y = 0. \quad (6.37)$$

Since  $(x, y)$  is an interior critical zero, (6.35) and (6.36) imply equation (6.38) below ; (6.35) and (6.37) imply equation (6.39) below.

$$\cos x \sin(Rx) - R \sin x \cos(Rx) = 0. \quad (6.38)$$

$$\cos y \sin(Ry) - R \sin y \cos(Ry) = 0. \quad (6.39)$$

Substituting  $\sin(Rx)$  and  $\sin(Ry)$  in (6.35) using (6.38) and (6.39), we obtain the equation

$$\cos x \cos(Ry) + \epsilon \cos(Rx) \cos y = 0. \quad (6.40)$$

Adding and subtracting (6.35) to/from (6.40), we obtain that an interior critical zero  $(x, y)$  of  $Z_{\pm}$  satisfies the system,

$$\begin{aligned} \cos(x - Ry) + \epsilon \cos(Rx - y) &= 0, \\ \cos(x + Ry) + \epsilon \cos(Rx + y) &= 0. \end{aligned} \quad (6.41)$$

• Case  $\epsilon = 1$ . Modulo  $2\pi$ , the system (6.41) is equivalent to

$$\begin{aligned} (a1) \ x - Ry &= \pi - Rx + y [2\pi] \text{ or } (b1) \ x - Ry = \pi + Rx - y [2\pi], \\ &\text{and} \\ (a2) \ x + Ry &= \pi - Rx - y [2\pi] \text{ or } (b2) \ x + Ry = \pi + Rx + y [2\pi]. \end{aligned} \quad (6.42)$$

We have to consider four cases.

✓ (a1) & (a2) These conditions imply that  $Rx = -x + k\pi$  for some integer  $k$ . Using (6.38), we find that

$$(-1)^{k+1}(1 + R) \sin x \cos x = 0.$$

This implies that  $x = \pi/2$ . Similarly, using (6.39), we find that  $y = \pi/2$ . Since  $(x, y)$  is a critical zero, using Subsection 6.1, this can only occur when  $R$  is odd. On the other hand, using (6.35), we find that  $\sin(R\pi/2) = 0$  which implies that  $R$  is even. The conditions (a1) and (a2) cannot occur simultaneously.

✓ (a1) & (b2) These conditions imply that  $x = y$ . Using (6.35), we find that  $\sin(Rx) = 0$  and hence, by (6.38),  $\cos(Rx) = 0$ . The conditions (a1) and (b2) cannot occur simultaneously.

✓ (b1) & (a2) These conditions imply that  $y = \pi - x$ . Using (6.35), we see that

$$((-1)^{R+1} + 1) \sin x \sin(Rx) = 0.$$

If  $R$  were odd, we would have a contradiction with (6.38). This case can only occur when  $R$  is even.

✓ (b1) & (b2) These conditions imply that  $Rx = x + k\pi$  for some integer  $k$ . By (6.38), this implies that  $x = \pi/2$ . Similarly, we find that  $y = \pi/2$ . As above, this implies that  $R$  is odd. On the other-hand, (6.35), implies that  $\sin(R\pi/2)$  which implies that  $R$  is even. The conditions (b1) and (b2) cannot occur simultaneously.

We conclude that the function  $Z_+$  has no interior critical zero when  $R$  is odd, and that its only critical zeroes are the points  $(q_i, \pi - q_i)$ , for  $1 \leq i \leq R - 2$  when  $R$  is even.

• Case  $\epsilon = -1$ . The system (6.41) is equivalent to

$$\begin{aligned} (a1) \quad x - Ry = Rx - y [2\pi] \text{ or } (b1) \quad x - Ry = -Rx + y [2\pi], \\ \text{and} \\ (a2) \quad x + Ry = Rx + y [2\pi] \text{ or } (b2) \quad x + Ry = -Rx - y [2\pi]. \end{aligned} \tag{6.43}$$

We have to consider four cases.

✓ (a1) & (a2) These conditions imply that  $Rx = x + k\pi$  for some integer  $k$ . Using (6.38), we find that

$$(-1)^{k+1}(1 - R) \sin x \cos x = 0.$$

This implies that  $x = \pi/2$ . Similarly, using (6.39), we find that  $y = \pi/2$ . Since  $(x, y)$  is a critical zero, using Subsection 6.1, this case can only occur when  $R$  is odd.

✓ (a1) & (b2) These conditions imply that  $\pi - x = y$ . Using (6.35), we find that

$$((-1)^{R+1} - 1) \sin(Rx) = 0.$$

Since  $(x, y)$  is a critical zero,  $\sin(Rx) \neq 0$  and this case can only occur when  $R$  is odd.

✓ (b1) & (a2) These conditions imply that  $y = x$ . This case occurs for both  $R$  even and  $R$  odd.

✓ (b1) & (b2) These conditions imply that  $Rx = -x + k\pi$  for some integer  $k$ . By (6.38), this implies that  $x = \pi/2$ . Similarly, we find that  $y = \pi/2$ . This case can only occur when  $R$  is odd.

We conclude that the only critical zeroes of the function  $Z_-$  are the points  $(q_i, q_i)$ , for  $1 \leq i \leq R - 2$  when  $R$  is even, and are the points,  $(q_i, q_i)$ ,  $(q_i, \pi - q_i)$ , for  $1 \leq i \leq R - 2$  when  $R$  is odd.  $\square$

Recall that the function  $Z_+(x, y)$  satisfies the relations

$$Z_+(y, x) = Z_+(x, y) \quad \text{and} \quad Z_+(\pi - x, \pi - y) = (-1)^{R+1} Z_+(x, y)$$

which imply that the nodal set  $N(Z_+)$  is invariant under the symmetry with respect to the diagonal  $\mathcal{D}_+$ , and under the symmetry with respect to the centre  $O$  of the square  $\mathcal{S}$ . Consider the subsets

$$\begin{aligned} \mathcal{F}_1 &:= \{\mathcal{S} \cap \{x > y\} \cap \{x + y < \pi\}\}, \\ \mathcal{F}_2 &:= \{\mathcal{S} \cap \{x > y\} \cap \{x + y > \pi\}\}, \\ \mathcal{F}_3 &:= \{\mathcal{S} \cap \{x < y\} \cap \{x + y > \pi\}\}, \\ \mathcal{F}_4 &:= \{\mathcal{S} \cap \{x < y\} \cap \{x + y < \pi\}\}. \end{aligned} \tag{6.44}$$

Due to the symmetries mentioned above, it suffices to understand the nodal set into one of these domains. Since  $Z_+$  corresponds to the value  $\theta = \pi/4$ , the diagonal  $\mathcal{D}_+$  is covered by grey  $Q$ -squares. When  $R$  is even, the anti-diagonal  $\mathcal{D}_-$  is covered by white squares which either contain a unique critical zero of  $Z_+$ , or have as vertex one of the vertices  $(0, \pi)$  or  $(\pi, 0)$ . In either situations, the structure of  $N(Z_+)$  inside these diagonal white  $Q$ -squares is known, see Section 6.4. When  $R$  is odd, both diagonals  $\mathcal{D}_+$  and  $\mathcal{D}_-$  are covered by grey squares, and the white  $Q$ -squares meeting a given  $\mathcal{F}_i$  are actually contained in  $\mathcal{F}_i$ . In summary, it suffices to understand the nodal pattern of  $Z_+$  inside the white squares contained into the  $\mathcal{F}_i$ , and it suffices to look at the case  $i = 1$ , and use the symmetries.

**Claim.** *In each white square  $Q_{i,j} \subset \mathcal{W}(+) \cap \mathcal{F}_1$ , the horizontal segment  $]p_i, p_{i+1}[ \times \{m_j\}$  does not meet the nodal set  $N(Z_+)$ . More precisely, for  $R = 2r$  and  $j \leq r - 1$ ,*

$$(-1)^j Z_+(x, m_j) > 0 \text{ on the interval } ]p_{j+1}, \pi - p_{j+1}[.$$

**Proof.** Since  $Q_{i,j} \in \mathcal{W}(+)$ , we must have  $i + j$  odd i.e.,  $(-1)^{i+j} = -1$ . Since  $Q_{i,j} \subset \mathcal{F}_1$ , we must have the inequalities  $j \leq i - 1$  and  $i + j \leq R - 2$ . Up to the positive factor  $1/\sqrt{2}$ , we have, for any  $x \in ]p_i, p_{i+1}[$ ,

$$\begin{aligned} Z_+(x, m_j) &= \sin x \sin(Rm_j) + \sin(Rx) \sin m_j \\ &= (-1)^j (\sin x + (-1)^j \sin m_j \sin(Rx)) \\ &= (-1)^j (\sin x - \sin m_j |\sin(Rx)|), \end{aligned} \tag{6.45}$$

where the last equality follows from the equalities  $\sin(Rx) = (-1)^i |\sin(Rx)|$  on the interval  $]p_i, p_{i+1}[$ , and  $(-1)^{i+j} = -1$ . On the other-hand, the inequalities  $j \leq i - 1$  and  $i + j \leq R - 2$  imply that  $m_j < p_i < p_{i+1} < \pi - m_j$ , so that  $\sin x > \sin m_j$  on  $]p_i, p_{i+1}[$ . This proves that  $Z_+(x, m_j) \neq 0$  on  $]p_i, p_{i+1}[$ , hence the claim.  $\square$ .

Taking into account the preceding discussion, we have obtained the following lemma.

**Lemma 6.8** *The horizontal segments (medians) through the points  $(m_i, m_j)$  which are contained in the white squares  $Q_{i,j} \subset \mathcal{W}(+) \cap \mathcal{F}_1$  or  $\mathcal{W}(+) \cap \mathcal{F}_3$  do not meet the nodal set  $N(Z_+)$ . The vertical segments (medians) through  $(m_i, m_j)$  which are contained in the white squares  $Q_{i,j} \subset \mathcal{W}(+) \cap \mathcal{F}_2$  or  $\mathcal{W}(+) \cap \mathcal{F}_4$  do not meet the nodal set  $N(Z_+)$ .*

We have a similar lemma for the eigenfunction  $Z_-$ .

**Lemma 6.9** *The horizontal segments (medians) through  $(m_i, m_j)$  which are contained in the white squares  $Q_{i,j} \subset \mathcal{W}(+) \cap \mathcal{F}_1$  or  $\mathcal{W}(-) \cap \mathcal{F}_3$  do not meet the nodal set  $N(Z_-)$ . The vertical segments (medians) through  $(m_i, m_j)$  which are contained in the white squares  $Q_{i,j} \subset \mathcal{W}(+) \cap \mathcal{F}_2$  or  $\mathcal{W}(+) \cap \mathcal{F}_4$  do not meet the nodal set  $N(Z_-)$ .*

**Proof.** We sketch the proof of the lemma. Since  $N(Z_+)$  and  $N(Z_-)$  are symmetrical to each other with respect to  $\{x = \pi/2\}$  when  $R$  is even, it suffices to study  $N(Z_-)$  for  $R$  odd. The nodal set is contained in  $\mathcal{W}(-)$ . The diagonal and the anti-diagonal are covered by white  $Q$ -squares, and in these squares the nodal pattern is known since they either contain a critical zero or touch a vertex of the square  $\mathcal{S}$ . As above, we look at the white squares inside  $\mathcal{F}_1$ . The indices of these squares satisfy

$$(-1)^{i+j} = 1, \quad j \leq i - 1, \quad i + j \leq R - 2.$$



As in the previous proof, we can write,

$$\begin{aligned}
Z_-(x, m_j) &= \sin x \sin(Rm_j) - \sin(Rx) \sin m_j \\
&= (-1)^j (\sin x + (-1)^j \sin m_j \sin(Rx)) \\
&= (-1)^j (\sin x - \sin m_j |\sin(Rx)|),
\end{aligned} \tag{6.46}$$

because  $\sin(Rx) = (-1)^i |\sin(Rx)|$  in the interval  $]p_i, p_{i+1}[$ , and  $(-1)^{i+j} = 1$ .

The same argument as above gives that the horizontal median  $]p_i, p_{i+1}[\times\{m_j\}$  does not meet  $N(Z_-)$ .  $\square$

**Remark.** Similar lemmas hold with the horizontal and vertical segments  $]p_i, p_{i+1}[\times\{q_j\}$  and  $\{q_i\}\times]p_j, p_{j+1}[$ .

**Proof of Proposition 6.6.** The idea of the proof is to follow the nodal set along the boundary of each square  $\partial\mathcal{S}_i$ , with  $i = 1, 2, \dots, r$  (say from the point  $(p_i, p_i)$  anticlockwise, through  $(p_{R-i}, p_i)$ ,  $(p_{R-i}, p_{R-i})$ ,  $(p_i, p_{R-i})$ , and back to  $(p_i, p_i)$ ), and to use the properties of the functions  $Z_{\pm}$  (no critical zeroes on the open edges, known nodal patterns at the vertices, known interior critical zeroes, and their localization together with Lemmas 6.8 and 6.9).

When  $R = 2r$  is even, it suffices to prove the result for  $Z_+$ . We already know that the nodal set of  $Z_+$  contains the anti-diagonal and  $\partial\mathcal{S}$ . Start from  $(p_1, p_1)$  horizontally. The absence of critical zero on the edge  $]0, \pi[\times\{0\}$  and Lemma 6.8 tell us that the nodal line can only intertwine the edge of  $\mathcal{S}_1$  until it enters the square  $Q_{1, 2r-2}$  at the point  $(p_1, p_{2r-2})$ . Due to the nodal pattern in this square which contains the critical zero  $(q_1, \pi - q_1)$ , the nodal line exits the square at the point  $(p_{R-1}, p_2)$ . By Lemma 6.8, and the absence of critical zero on the edge  $\{\pi\}\times]0, \pi[$ , the nodal line has to follow upwards along  $x = p_{R-1}$ , till the point  $(p_{R-1}, p_{R-1})$  where there is no choice but to get along the horizontal edge at this point, backwards until the nodal line enters  $Q_{1, R-2}$  at the point  $(p_2, p_{R-1})$ . In this square, the nodal pattern is known, and the nodal line has to leave through the point  $(p_1, p_{R-2})$  downwards along the last edge of  $\mathcal{S}_1$  back to the starting point. This is the first closed curve  $\gamma_1$ . We can now iterate the procedure along  $\mathcal{S}_2$ , using Lemma 6.8 to constrain the nodal set from both sides. After  $(r - 1)$  iterations, we end up with  $(r - 1)$  closed curves, and we have visited every point in  $\mathcal{L}$  (if we take the diagonal into account). The curves  $\gamma_i$  cannot meet because an intersection point would be a critical zero, and we know that the only critical zeroes of  $Z_+$  are on the anti-diagonal. The nodal set cannot contain any other connected component, otherwise such a component would be entirely contained in a white  $Q$ -square, and we know that this is not possible for energy reasons. This proves Assertion (i).

We obtain the other assertions by similar arguments.  $\square$

**Remark.** We have just proved that the nodal patterns of  $Z_{\pm}$  are as suggested by the pictures (see Figures 6.9, 6.10, and 6.11).

## 6.6 Deformation of nodal patterns

In this subsection, we investigate how nodal patterns of the family of eigenfunctions  $\{\Phi^{\theta}\}$  evolve when the parameter  $\theta$  varies.

**Lemma 6.10** *Assume  $\theta$  is not a critical value of the parameter, i.e., does not belong to the set  $\mathcal{T} := \mathcal{T}_o \cup \mathcal{T}_x \cup \mathcal{T}_y$ .*

- (i) The patterns (A) and (B) in Figure 6.4, and the patterns (A), (C) and (D) in Figures 6.5 or 6.6, are stable in any interval  $]\theta - \epsilon, \theta + \epsilon[ \subset \mathcal{T}$ .
- (ii) Let  $\theta_k \in \mathcal{T}_o$  be some critical value of  $\theta$ . When  $\theta$  is close to  $\theta_k$  and  $\theta > \theta_k$  (resp.  $\theta < \theta_k$ ), the pattern (C) in Figure 6.4 changes to one of the patterns (A) or (B) (resp. (B) or (A)).
- (iii) Let  $\theta_k \in \mathcal{T}_x \cup \mathcal{T}_y$  be some critical value of  $\theta$ . When  $\theta$  is close to  $\theta_k$  and  $\theta > \theta_k$  (resp.  $\theta < \theta_k$ ), the patterns (B) in Figures 6.5 or 6.6 change to one of the patterns (C) or (D) (resp. (D) or (C)).

**Remark.** The proof provides more information than the above statement.

**Proof.** The proofs are similar for  $R$  even and  $R$  odd. We only sketch the proofs for  $R$  even. *Assertion (i).* Assume we are in a square  $Q_{i,j}$  which does not touch the boundary of the square. In order to prove the first assertion, we consider the segment  $]0, \pi[\times\{q_j\} \cap Q_{i,j}$  for the patterns Figure 6.4 (A), and the segment  $\{q_i\} \times ]0, \pi[ \cap Q_{i,j}$  for the pattern Figure 6.4 (B). The argument is the same in the two cases. Let us consider the last one. The function  $y \rightarrow \Phi(q_i, y, \theta)$  has precisely two simple zeroes in the interval  $]p_j, p_{j+1}[$ . The function  $y \rightarrow \Phi(q_i, y, \theta')$  will still have two simple zeroes for  $\theta'$  close to  $\theta$ . As a matter of fact, when  $\theta'$  varies, the two arcs of nodal set become closer and closer, and eventually touch, which occurs precisely when  $\theta'$  reaches a critical value in  $\mathcal{T}_o$ .

*Assertion (ii).* We consider some critical value  $\theta_k$ , and use the same segments as in the proof of the first assertion. There are two cases for  $\Phi(x, y, \theta_k)$  in the square  $Q_{i,j}$ : it is non negative on the vertical segment and non positive on the horizontal one, or vice and versa. Both cases are dealt with in the same manner. For symmetry reasons, we can also assume that  $0 < \theta < \pi/4$ , so that the nodal set meets  $Q_{i,j}$  if and only if  $(-1)^{i+j} = -1$ . For  $\theta$  close to and different from  $\theta_k$ , we write,

$$\begin{aligned} \Phi(q_i, y, \theta) &= \Phi(q_i, y, \theta_k) \\ &+ (-1)^j \left( (\cos \theta - \cos \theta_k) \sin q_i (-1)^j \sin(Ry) \right. \\ &\quad \left. - (\sin \theta - \sin \theta_k) (-1)^i \sin(Rq_i) \sin y \right). \end{aligned} \quad (6.47)$$

Assuming that  $\Phi(q_i, y, \theta_k) \geq 0$  inside the square  $Q_{i,j}$  and looking at signs, we then see that  $\Phi(q_i, y, \theta) > 0$  inside  $Q_{i,j}$  if either  $j$  is even and  $\theta < \theta_k$ , or  $j$  is odd and  $\theta > \theta_k$ . This means that the nodal pattern Figure 6.4 (C) evolves to the nodal pattern Figure 6.4 (A) in these cases. Similarly, we write

$$\begin{aligned} \Phi(x, q_j, \theta) &= \Phi(x, q_j, \theta_k) \\ &+ (-1)^j \left( (\cos \theta - \cos \theta_k) \sin x (-1)^j \sin(Rq_j) \right. \\ &\quad \left. - (\sin \theta - \sin \theta_k) (-1)^i \sin(Rx) \sin q_j \right). \end{aligned} \quad (6.48)$$

Assuming that  $\Phi(x, q_j, \theta_k) \leq 0$  inside the square  $Q_{i,j}$ , and looking at signs, we see that  $\Phi(x, q_j, \theta) < 0$  inside  $Q_{i,j}$  if either  $j$  is even and  $\theta > \theta_k$ , or  $j$  is odd and  $\theta < \theta_k$ . This means that the nodal pattern Figure 6.4 (C) evolves to the nodal pattern Figure 6.4 (B) in these cases.

*Assertion (iii).* The proof is similar to the proof of Assertion (ii). □

## 6.7 Desingularization of $Z_+$

In this subsection, we study how the nodal set of the eigenfunction  $\{\Phi^\theta\}$  changes when  $\theta$  varies in a small neighborhood of  $\pi/4$ , while  $(x, y)$  lies in the neighborhood of a critical zero of the eigenfunction  $Z_+$ . Since  $Z_+$  has no critical zero when  $R = 2r + 1$ , we only consider the case  $R = 2r$ .

Recall the results and notations of Subsection 6.1. By Lemma 6.7, the critical zeros of  $Z_+$  are the points  $(q_i, \pi - q_i)$ ,  $1 \leq i \leq R - 2$ . Take into account the fact that  $R$  is even, and hence that  $U_{R-1}$  is odd. For  $(x, y)$  in the square  $Q(i) := Q_{i, 2r-1-i}$  which contains the point  $(q_i, \pi - q_i)$ , write

$$\begin{aligned}\sqrt{2} Z_+(q_i, y) &= \sin q_i \sin y (-1)^i |U_{R-1}(\cos y) + M_i|, \\ \sqrt{2} Z_+(x, \pi - q_i) &= \sin q_i \sin x (-1)^{i+1} |U_{R-1}(\cos x) - M_i|,\end{aligned}\tag{6.49}$$

where  $M_i$  is defined in Properties 6.1(v). These equations give the local nodal pattern for the eigenfunction  $Z_+$  in the square  $Q(i)$ . When  $i$  is odd, *resp.* even, the nodal pattern is given by Figure 6.7 (i), *resp.* by Figure 6.7 (ii).

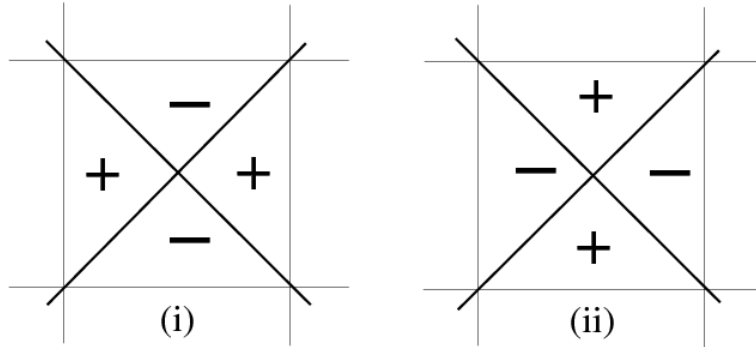


Figure 6.7: Local nodal patterns at an interior critical zero

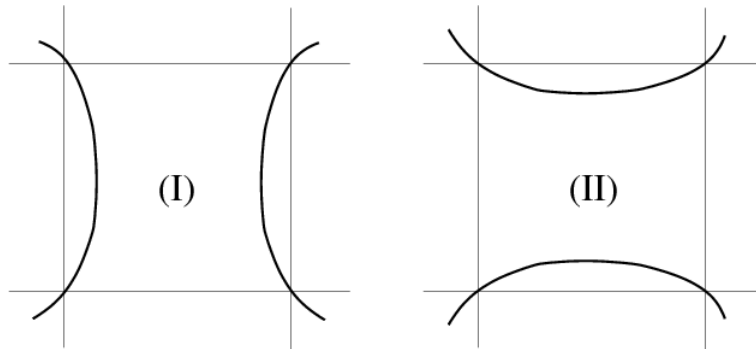


Figure 6.8: Local nodal patterns in the absence of critical zero

On the other hand, we can write,

$$\begin{aligned}\Phi(q_i, y, \theta) &= \sin q_i \sin y \left\{ \cos \theta \sqrt{2} Z_+(q_i, y) + (\sin \theta - \cos \theta) M_i \right\} \\ &= (-1)^i \left\{ \cos \theta \sqrt{2} |Z_+(q_i, y)| - \sin q_i \sin y (\sin \theta - \cos \theta) |M_i| \right\}.\end{aligned}\tag{6.50}$$

The last factor in the second line of (6.50) is positive when  $0 < \pi/4 - \theta \ll 1$ . It follows that the local pattern of the nodal set  $N(\Phi)$  inside  $Q(i)$ , is given by Figure 6.8 (II).

Similarly, we can write

$$\begin{aligned}\Phi(x, \pi - q_i, \theta) &= \sin q_i \sin x \left\{ \sin \theta \sqrt{2} Z_+(x, \pi - q_i) + (\sin \theta - \cos \theta) M_i \right\} \\ &= (-1)^{i+1} \left\{ \sin \theta \sqrt{2} |Z_+(x, \pi - q_i)| + \sin q_i \sin y (\sin \theta - \cos \theta) |M_i| \right\}.\end{aligned}\quad (6.51)$$

The last factor in the second line of (6.51) is positive when  $0 < \theta - \pi/4 \ll 1$ . It follows that the local nodal pattern of the nodal set  $N(\Phi^\theta)$  inside  $Q(i)$ , is given by Figure 6.8 (I).

**Remark.** Notice that the pattern is independent of  $i$ . When  $\theta$  leaves the value  $\pi/4$ , all the critical zeroes of the eigenfunction  $Z_+$  disappear at once, and the local nodal patterns of  $\Phi^\theta$  in the  $Q$ -squares containing the critical zeroes of  $Z_+$  look alike, opening “horizontally” as in Figure 6.8 (II), when  $\theta < \pi/4$ ; *resp.* opening “vertically” as in Figure 6.8 (I), when  $\theta > \pi/4$ , as stated in Theorem 4.1 (ii).

## 6.8 Desingularization of $Z_-$

Since  $Z_+$  and  $Z_-$  are symmetrical with respect to  $\{x = \pi/2\}$  when  $R = 2r$ , we only have to consider the case  $R = 2r + 1$ . When  $R = 2r + 1$ , the interior critical zeroes of  $Z_-$  are the point  $(\pi/2, \pi/2)$  and the points  $(q_i, q_i)$ ,  $(q_i, \pi - q_i)$ , for  $1 \leq i \leq R - 2$ . Due to the symmetries with respect to  $\{x = \pi/2\}$  and  $\{y = \pi/2\}$ , it suffices to consider the points  $(q_i, q_i)$ ,  $1 \leq i \leq r$ , and the square  $Q_{i,i}$ .

We can write

$$\begin{aligned}\sqrt{2} Z_-(q_i, y) &= \sin q_i \sin y (-1)^{i+1} |U_{R-1}(\cos y) - M_i|, \\ \sqrt{2} Z_-(x, q_i) &= \sin q_i \sin x (-1)^i |U_{R-1}(\cos x) - M_i|.\end{aligned}\quad (6.52)$$

These equations give the local nodal pattern for the eigenfunction  $Z_-$  in the square  $Q_{i,i}$ . When  $i$  is even, *resp.* odd, the pattern is given by Figure 6.7 (i), *resp.* by Figure 6.7 (ii).

On the other hand, we can write,

$$\begin{aligned}\Phi(q_i, y, \theta) &= \cos \theta \sqrt{2} Z_-(q_i, y) + \sin q_i \sin y (\sin \theta + \cos \theta) M_i \\ &= (-1)^i \left\{ |\cos \theta \sqrt{2} Z_-(q_i, y)| + \sin q_i \sin y (\sin \theta + \cos \theta) |M_i| \right\}.\end{aligned}\quad (6.53)$$

The last factor in the second line of (6.53) is positive when  $0 < 3\pi/4 - \theta \ll 1$ . It follows that the local pattern of the nodal set  $N(\Phi^\theta)$ , is given by Figure 6.8 (I).

Similarly, we can write

$$\begin{aligned}\Phi(x, q_i, \theta) &= -\sin \theta \sqrt{2} Z_-(x, q_i) + \sin q_i \sin x (\sin \theta + \cos \theta) M_i \\ &= (-1)^{i+1} \left\{ \sin \theta \sqrt{2} |Z_-(x, q_i)| - \sin q_i \sin y (\sin \theta + \cos \theta) |M_i| \right\}.\end{aligned}\quad (6.54)$$

The last factor in the second line of (6.54) is positive when  $0 < \theta - 3\pi/4 \ll 1$ . It follows that the local pattern of the nodal set  $N(\Phi^\theta)$ , is given by Figure 6.8 (II).

We point out that the pattern is independent of the sign of  $i$ . When  $\theta$  leaves the value  $3\pi/4$ , all the critical zeroes of the eigenfunction  $Z_-$  disappear at once, and the local nodal patterns of  $\Phi^\theta$  in the squares containing the critical zeroes of  $Z_-$  look alike, opening “vertically” as in Figure 6.8 (I), when  $\theta < 3\pi/4$ ; *resp.* opening “horizontally” as in Figure 6.8 (II), when  $\theta > 3\pi/4$ .

## 6.9 The nodal pattern of $\Phi^\theta$ for $\theta$ close to $\pi/4$ and $R$ even

By Properties 6.2 (iv), we can assume that  $\theta \in [0, \pi/4]$ . We know from Properties 6.3, 6.4 and 6.5 that for  $R = 2r$  and  $0 < \pi/4 - \theta \ll 1$ , the eigenfunction  $\Phi^\theta$  has no interior critical zero, two non degenerate edge critical zeroes, respectively in the intervals  $\{0\} \times ]p_{R-1}, \pi[$  and  $\{\pi\} \times ]0, p_1[$ , and that the vertices are non degenerate critical zeroes.

Using Lemma 6.10, the nodal pattern of  $N(\Phi^\theta)$  for  $\theta$  close to  $\pi/4$ , is the same as the nodal pattern of  $Z_+$  in the  $Q$ -squares without critical zero, namely the white  $Q$ -squares which do not meet the anti-diagonal. To determine the nodal set of  $N(\Phi^\theta)$ , it suffices to know the local nodal patterns in the white  $Q$ -squares covering the anti-diagonal. This is given by Subsection 6.7, *the crosses at an interior critical zero open up horizontally*, and by the description of the critical zeroes on the vertical edges near the vertices  $(0, \pi)$  and  $(\pi, 0)$ . It is now clear that the nodal set of  $\Phi^\theta$  for  $\theta$  close enough to  $\pi/4$  is connected, and divides the square into two connected components.

**Remark.** As the diaporama of subfigures in Figure 6.9 shows, there is another way to obtain examples of eigenfunctions with exactly two domains, using a deformation of one of the simplest product eigenfunctions. The following figures display the nodal sets for the eigenfunctions  $\Phi_{1,8}^\theta$  and  $\Phi_{1,9}^\theta$ . The values of  $\theta$  appear in the title. The values with more than two digits correspond to the critical values of the parameter, i.e., the values of  $\theta$  for which critical zeroes or equivalently multiple points appear/disappear in the nodal set, see (6.19) and (6.20). The values with two digits are intermediate values between two consecutive critical values. The topology of the nodal set does not change in such intervals.

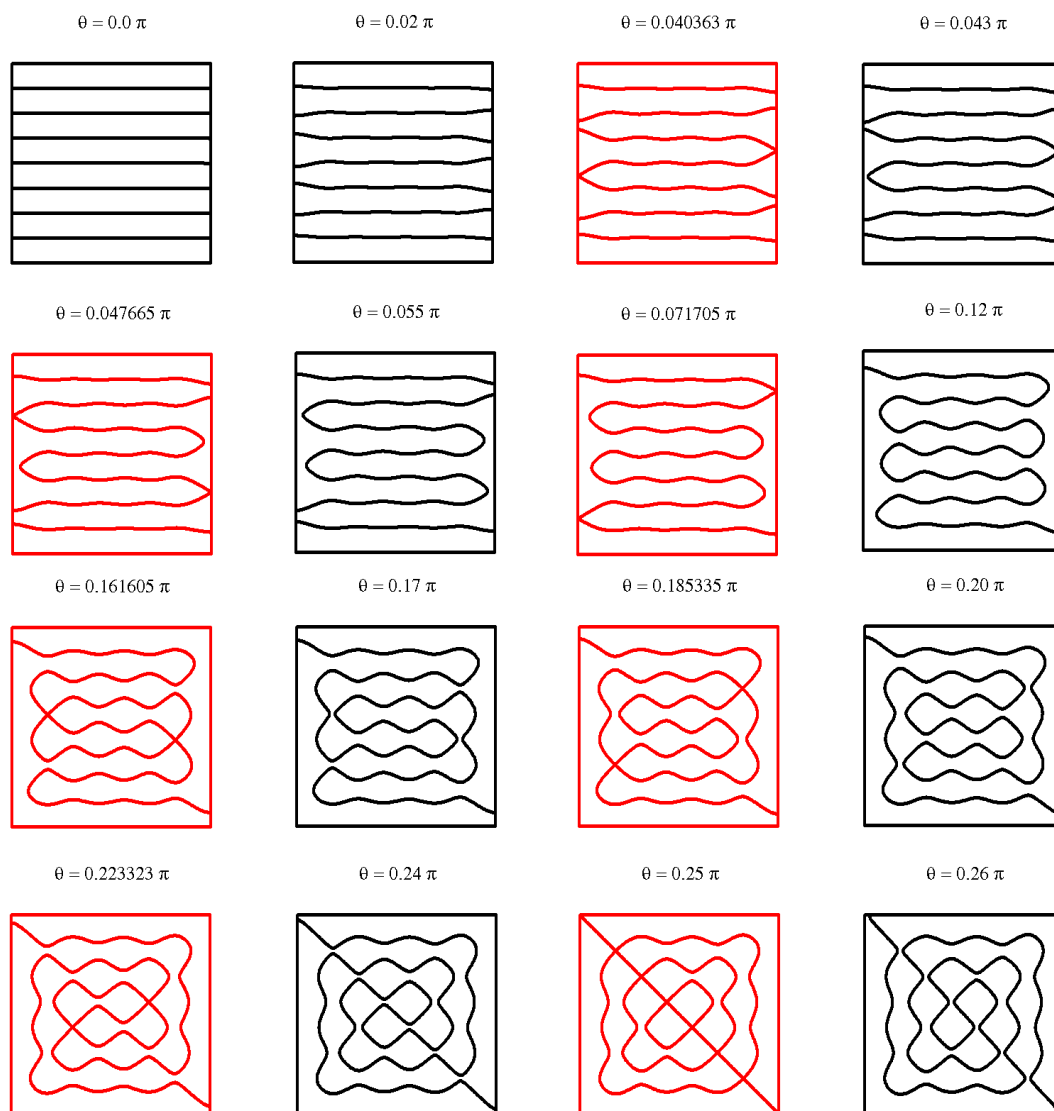


Figure 6.9: Typical nodal patterns for the eigenvalue  $(1, 8)$

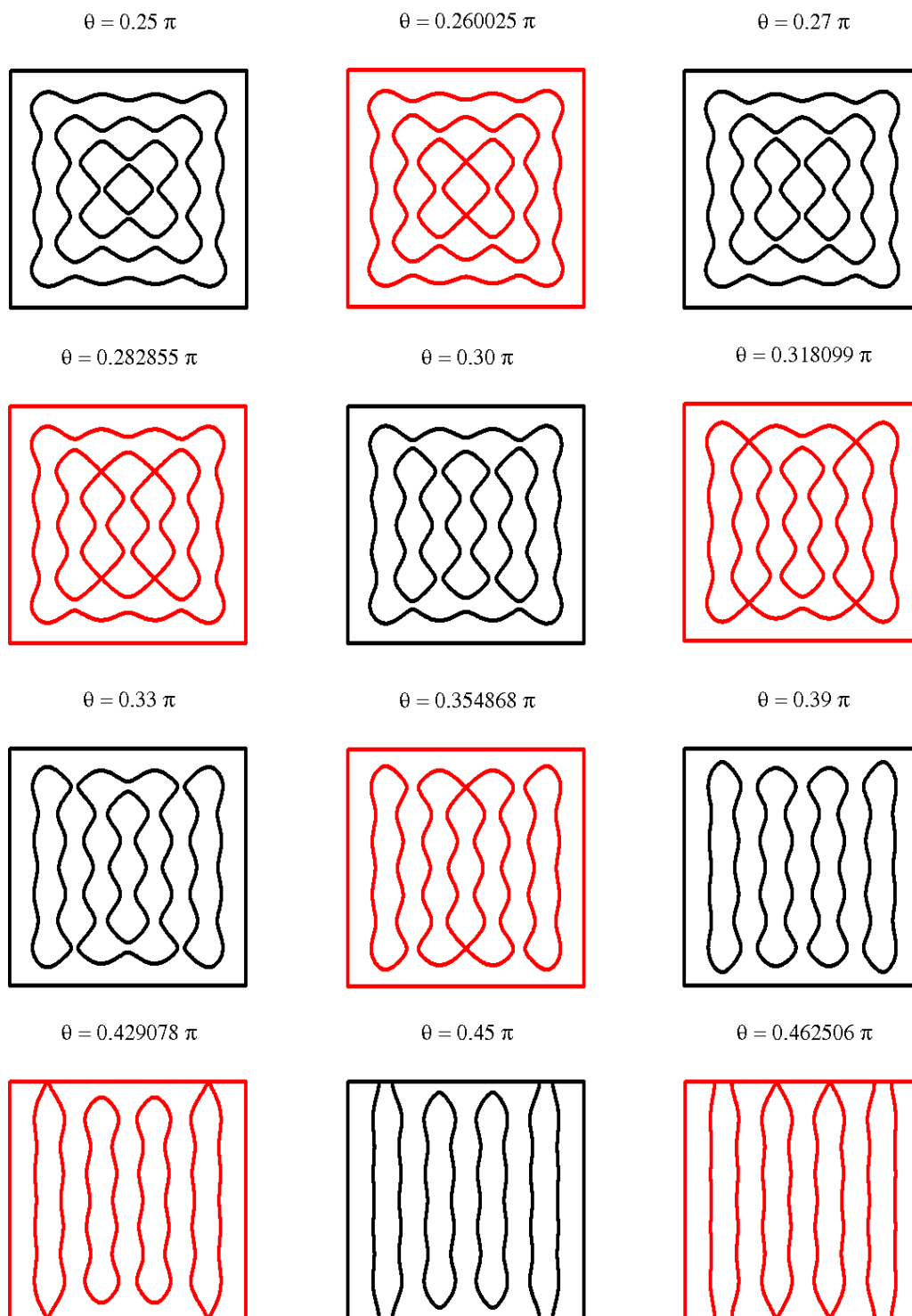


Figure 6.10: Typical nodal patterns for the eigenvalue  $(1, 9)$

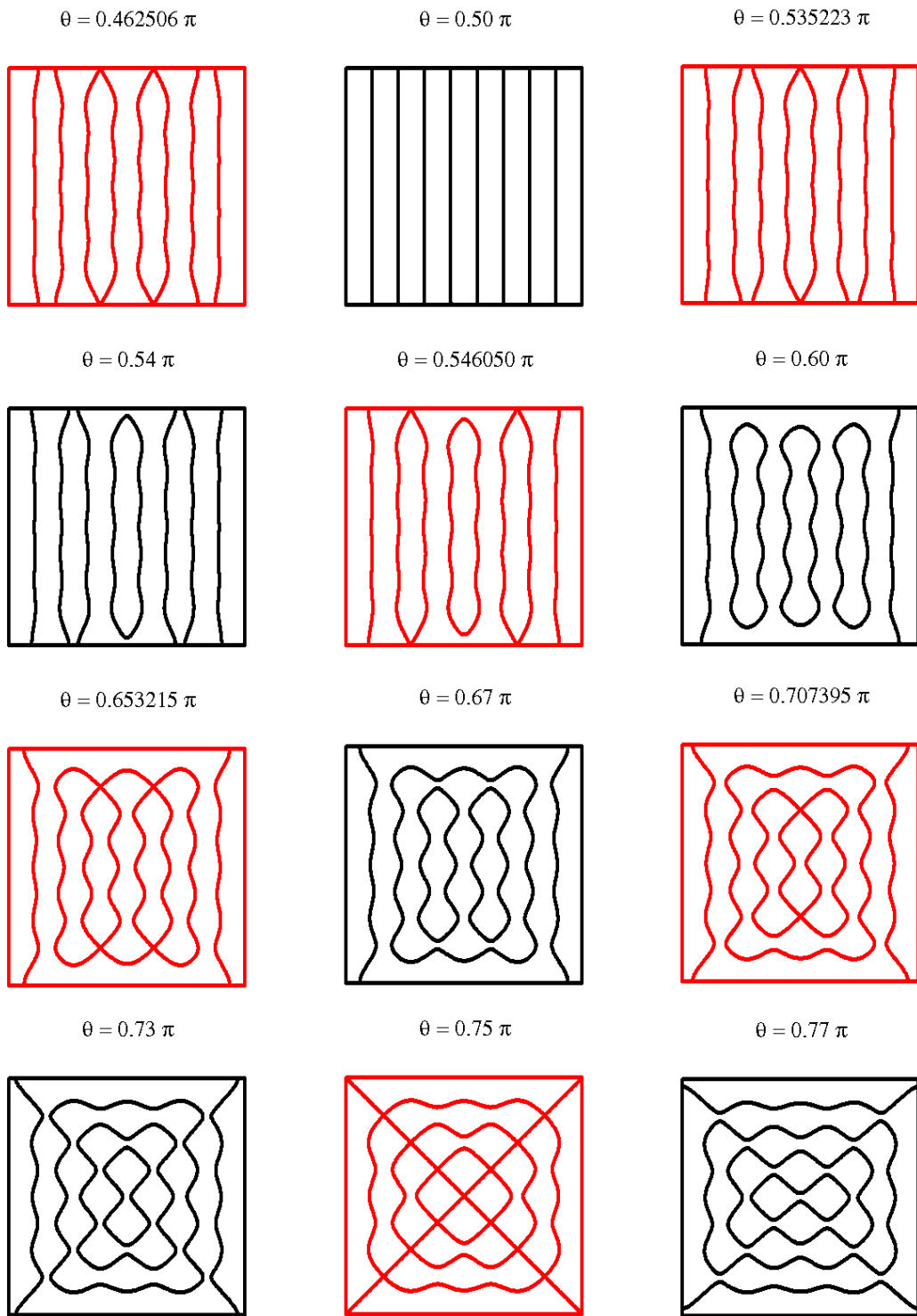


Figure 6.11: Typical nodal patterns for the eigenvalue  $(1, 9)$ , continued



## References

- [1] C. Bandle. Isoperimetric Inequalities and Applications. Pitman Publishing Inc., 1980.
- [2] P. Bérard. Inégalités isopérimétriques et applications. Domaines nodaux des fonctions propres. SEDP (Polytechnique) (1981-1982) Exposé 11. [http://www.numdam.org/item?id=SEDP\\_1981-1982\\_\\_\\_\\_A10\\_0](http://www.numdam.org/item?id=SEDP_1981-1982____A10_0)
- [3] P. Bérard and B. Helffer. A. Stern’s analysis of the nodal sets of some families of spherical harmonics revisited. arXiv:1407.5564.
- [4] P. Bérard and D. Meyer. Inégalités isopérimétriques et applications. Ann. Sci. École Norm. Sup. **15** (1982), 513-541.
- [5] V. Bonnaillie-Noël. Pictures of nodal domains for the square with Dirichlet boundary conditions. <http://www.math.ens.fr/~bonnaillie/Simulations/LaplacienCarre/LapCarre.html>
- [6] R. Courant. Ein allgemeiner Satz zur Theorie der Eigenfunktionen selbstadjungierter Differentialausdrücke, Nachr. Ges. Göttingen (1923), 81-84.
- [7] R. Courant and D. Hilbert. Methods of Mathematical Physics, Vol. 1. New York 1953.
- [8] R. Courant and D. Hilbert. Methoden der Mathematischen Physik I. Dritte Auflage. Heidelberger Taschenbücher Band 30. Springer 1968.
- [9] Rayleigh-Faber-Krahn. Encyclopedia of Mathematics. [http://www.encyclopediaofmath.org/index.php?title=Rayleigh-Faber-Krahn\\_inequality&oldid=22969](http://www.encyclopediaofmath.org/index.php?title=Rayleigh-Faber-Krahn_inequality&oldid=22969)
- [10] G. Gauthier-Shalom and K. Przytycki. Description of a nodal set on  $\mathbb{T}^2$ . 2006 McGill University Research Report (unpublished).
- [11] B. Helffer, T. Hoffmann-Ostenhof. A review on large  $k$  minimal spectral  $k$ -partitions and Pleijel’s Theorem. To appear in the proceedings of the 2013 conference in honor of J. Ralston.
- [12] B. Helffer, T. Hoffmann-Ostenhof, and S. Terracini. Nodal domains and spectral minimal partitions. Ann. Inst. H. Poincaré Anal. Non Linéaire **26** (2009), 101–138.
- [13] H. Lewy. On the minimum number of domains in which the nodal lines of spherical harmonics divide the sphere. Comm. Partial Differential Equations **2** (12) (1977), 1233–1244.
- [14] J. Leydold. On the number of nodal domains of spherical harmonics. Topology **35** (1996), 301–321.
- [15] W. Magnus, F. Oberhettinger and R.P. Soni. “Formulas and Theorems for the Special Functions of Mathematical Physics.” Third Edition. Berlin: Springer-Verlag, 1966.
- [16] J. Peetre. A generalization of Courant’s nodal domain theorem. Math. Scand. **5** (1957), 15–20.
- [17] Å. Pleijel. Remarks on Courant’s nodal theorem. Comm. Pure. Appl. Math. **9** (1956), 543–550.

- [18] F. Pockels. Über die partielle Differentialgleichung  $\Delta u + k^2 u = 0$  and deren Auftreten in mathematischen Physik. Historical Math. Monographs. Cornell University. (Originally Teubner- Leipzig 1891.) <http://ebooks.library.cornell.edu/cgi/t/text/text-idx?c=math;cc=math;view=toc;subview=short;idno=00880001>
- [19] A. Stern. Bemerkungen über asymptotisches Verhalten von Eigenwerten und Eigenfunktionen. Inaugural-Dissertation zur Erlangung der Doktorwürde der Hohen Mathematisch-Naturwissenschaftlichen Fakultät der Georg August-Universität zu Göttingen (30 Juli 1924). Druck der Dieterichschen Universitäts-Buchdruckerei (W. Fr. Kaestner). Göttingen, 1925.
- [20] A. Stern. Bemerkungen über asymptotisches Verhalten von Eigenwerten und Eigenfunktionen. Inaugural-Dissertation zur Erlangung der Doktorwürde der Hohen Mathematisch-Naturwissenschaftlichen Fakultät der Georg August-Universität zu Göttingen (30 Juli 1924). Extracts and annotations by P. Bérard and B. Helffer. <http://www-fourier.ujf-grenoble.fr/~pberard/R/stern-1925-thesis-partial-reprod.pdf>
- [21] A. Vogt. “Wissenschaftlerinnen in Kaiser-Wilhelm-Instituten. A-Z.” Veröffentlichungen aus dem Archiv zur Geschichte der Max-Planck-Gesellschaft, Bd. 12. Berlin 2008, 2. erw. Aufl.